PORTLAND PRESS

Research Article

Co-ordinated control of the ADP-heptose/ALPK1 signalling network by the E3 ligases TRAF6, TRAF2/c-IAP1 and LUBAC

Tom Snelling, Natalia Shpiro, Robert Gourlay, Frederic Lamoliatte and Philip Cohen

MRC Protein Phosphorylation and Ubiquitylation Unit, School of Life Sciences, University of Dundee, DD1 5EH Scotland, U.K.

Correspondence: Philip Cohen (p.cohen@dundee.ac.uk)

OPEN ACCESS

ADP-heptose activates the protein kinase ALPK1 triggering TIFA phosphorylation at Thr9, the recruitment of TRAF6 and the subsequent production of inflammatory mediators. Here, we demonstrate that ADP-heptose also stimulates the formation of Lys63- and Met1-linked ubiquitin chains to activate the TAK1 and canonical IKK complexes, respectively. We further show that the E3 ligases TRAF6 and c-IAP1 operate redundantly to generate the Lys63-linked ubiquitin chains required for pathway activation, which we demonstrate are attached to TRAF6, TRAF2 and c-IAP1, and that c-IAP1 is recruited to TIFA by TRAF2. ADP-heptose also induces activation of the kinase TBK1 by a TAK1-independent mechanism, which require TRAF2 and TRAF6. We establish that ALPK1 phosphorylates TIFA directly at Thr177 as well as Thr9 *in vitro*. Thr177 is located within the TRAF6-binding motif and its mutation to Asp prevents TRAF6 but not TRAF2 binding, indicating a role in restricting ADP-heptose signalling. We conclude that ADP-heptose signalling is controlled by the combined actions of TRAF2/c-IAP1 and TRAF6.

Introduction

The early detection of microbial pathogens is mediated via germline-encoded pattern recognition receptors (PRRs), which detect abundant and evolutionarily conserved molecules present in microbial pathogens that are absent or inaccessible in host cells, called pathogen-associated molecular patterns (PAMPs) [1]. The activation of PRRs triggers intracellular signal transduction pathways, which culminate in the generation of cytokines that mediate the host response to infection.

ADP-L,D-heptose and ADP-D,D-heptose are metabolites required for the incorporation of L, D-heptose and D,D-heptose into the inner and outer core of bacterial lipopolysaccharide (LPS), respectively [2]. D,D-heptose is also a constituent of S-layer glycoproteins present on the cell surface of archaea and bacteria [3], while septacidin and hygromycin B, which are secondary metabolites from Gram-positive bacteria, require ADP-LD-heptose and ADP-DD-heptose, respectively, for their biosynthesis [4]. In 2018, ADP-L,D-heptose and ADP-D,D-heptose (hereafter, ADP-heptose) were identified as activators of the atypical mammalian alpha-protein kinase 1 (ALPK1). The binding of ADP-heptoses to an N-terminal domain of ALPK1 induces an allosteric transition that activates the C-terminal kinase domain [5]. These investigators also showed that ADP-heptoses induced the activation of the transcription factor NF-κB and *IL-8* gene transcription in human embryonic kidney (HEK) 293 cells by a pathway that requires the expression of TNF receptor-activating factor (TRAF)-interacting protein with forkhead-associated (FHA) domain (TIFA) and TRAF6.

TIFA (comprising 184 amino acid residues) is a human FHA-containing protein that was identified in 2002 as a TRAF2-binding protein (T2BP) during a mammalian two-hybrid screen. Its overexpression in HEK293 cells was shown to activate the transcription factors NF-κB and AP-1 [6], and it was proposed to be a component of the TNF signalling pathway in which TRAF2 has a key role alongside TRAF5 [7]. Subsequently, T2BP was shown to interact with TRAF6 and renamed TIFA [8]. Based on

overexpression studies, TIFA was suggested to function as a scaffolding protein operating between IRAK1 and TRAF6 in MyD88-dependent signalling pathways [8] that are triggered by Interleukin-1 (IL-1) family members and by ligands that activate Toll-like receptors (TLRs). TIFA was also shown to stimulate the oligomerisation of TRAF6 and the activation of its E3 ligase activity [9].

FHA domains bind to phospho-threonine residues in proteins [10]. To identify sites of phosphorylation in TIFA, Huang and co-workers overexpressed FLAG-TIFA in HEK293 cells and after digestion with a cocktail of proteases that included GluC, as described elsewhere [11], identified Thr9 as one of several amino acid residues in TIFA that were phosphorylated [12]. Wild-type (WT) TIFA was shown to undergo self-oligomerisation through an intermolecular interaction between the FHA domain of one TIFA molecule and phospho-Thr9 of another; this did not occur if WT TIFA was replaced by the TIFA[T9A] mutant [12]. Other investigators also identified Thr9 as an amino acid residue in TIFA that became phosphorylated in response to heptose-1,7-bisphosphate (a precursor of ADP-heptose) in Jurkat cells [13]. At this time, the identity of the protein kinase that phosphorylated TIFA was unknown. Later, the ADP-heptose-dependent activation of NF-κB and *IL-8* gene transcription was found to be abolished when WT TIFA was replaced by the TIFA[T9A] mutant [5].

A variety of Gram-negative bacteria, including *Shigella flexneri*, *Salmonella enterica* Serovar Typhimurium, *Neisseria meningitidis* and *Helicobacteria pylori* induce the oligomerisation of TIFA in the gastric epithelial cell line AGS [2,14–16]. The cytokine deficiency-induced colitis susceptibility locus (*Cdcs1*), which is linked to mouse inflammatory bowel disease, also contains the *alpk1* gene. The *alpk1* gene is present in the genetic interval termed 'Hiccs' on mouse chromosome 3 that regulates *Helicobacter hepaticus*-induced colitis in a RAG1 KO background and leads to the eventual onset of colitis-associated colorectal cancer [17]. RAG1 KO mice develop colitis spontaneously upon infection with *H. hepaticus*, which is exacerbated in RAG1/ALPK1 double KO mice [18]. Intriguingly, the *alpk1* and *tifa* genes are adjacent on mouse chromosome 3, and the *ALPK1* and *TIFA* genes are adjacent on human chromosome 4. Here, we have performed a detailed biochemical and genetic analysis of the events that take place during the first hour of ADP-heptose-ALPK1-TIFA-signalling, which has revealed that TRAF2/c-IAP1 and TRAF6 both have critical roles in the regulation of this network.

Results

The ADP-heptose stimulated activation of MAP kinases and the canonical IKK complex requires ALPK1 and TIFA

In previous studies, the ADP-LD-heptose signalling pathway has been monitored in human embryonic kidney 293 (HEK293) cells by the activation of the transcription factor NF-κB using a luciferase reporter assay and by measuring *IL-8* transcript levels 4 h after the electroporation of 10 μM ADP-LD-heptose or the extracellular addition of 100 μM ADP-LD-heptose [5]. Here we monitored pathway activation routinely by the phosphorylation (activation) of the mitogen-activated protein kinases (MAPKs) p38α MAPK, p38γ MAPK and c-Jun N-terminal kinases 1 and 2 (JNK1/JNK2), and by the phosphorylation (activation) of the canonical IκB kinase (IKK) complex and its substrate NF-κB1 [19,20], and by the disappearance of its substrate IκBα from the cells. The IKKβ-catalysed phosphorylation of IκBα triggers its ubiquitylation by the E3 ligase SCF-β^{TRCP} causing its proteasomal degradation and activation of NF-κB [21]. Immunoblots with these antibodies are shown in Supplementary Figure S7 together with molecular mass markers so that their sizes can be gauged (Supplementary Figure S7).

We found that ADP-DD-heptose or ADP-LD-heptose activated the pathway near maximally when included in the culture medium at 10 μM (Supplementary Figure S1). ADP-DD-heptose (hereafter called ADP-heptose) was used for all subsequent experiments. Pathway activation in HEK293 cells (Figure 1A) or primary mouse bone marrow-derived macrophages (BMDM) (Figure 1B) was rapid, could be detected within 10 min and was maximal after 15–20 min. The strength of pathway activation induced by ADP-heptose in HEK293 cells was similar to that induced by IL-1β (Figure 1A) or in BMDM by R848, an activator of the Toll-like receptor 7/8 (TLR7/8) heterodimer (Figure 1B). The rapid ADP-heptose-stimulated destruction of IκBα was followed by its resynthesis within 45–60 min, because IκBα is an NF-κB-dependent gene (Figure 1A,B).

As expected, the knockout (KO) of ALPK1 or TIFA in HEK293 cells abolished ADP-heptose signalling (Figure 1C) but had no effect on IL-1β signalling (Supplementary Figure S2A). Interestingly, TIFA levels also decreased in a time-dependent manner following stimulation with ADP-heptose (Figure 1C).

It has been suggested that TIFA acts as a scaffold between IRAK1 and TRAF6 [8], but the KO of TIFA had no effect on IL-1β signalling (Supplementary Figure S2A) and the KO of IRAK1 had no effect on ADP-heptose
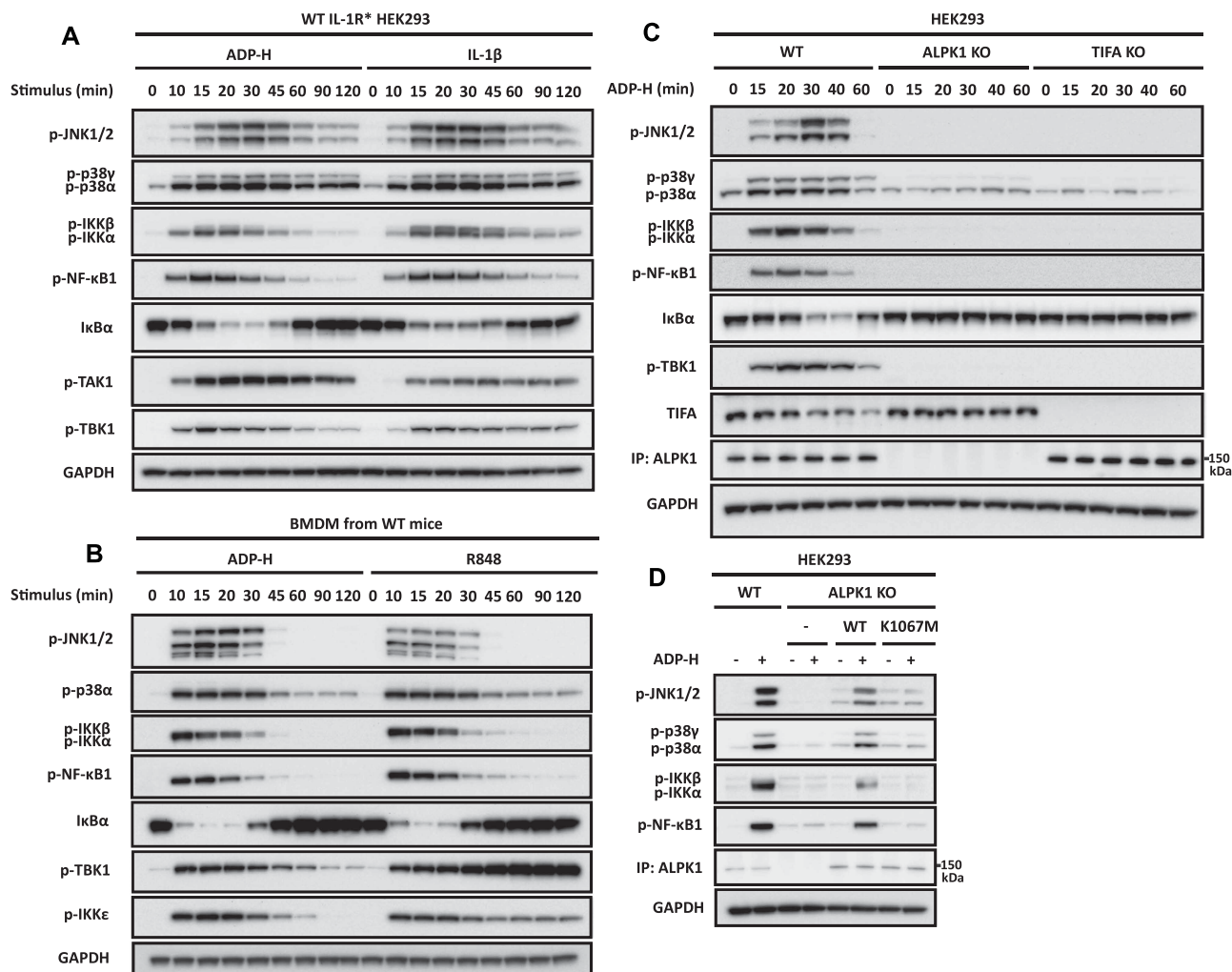
PORTLAND
PRESS

Figure 1. ADP-heptose induces the ALPK1- and TIFA-dependent activation of MAP kinases and the canonical IKK complex.
(A,B) IL-1R* HEK293 cells (A) or BMDM from wild-type (WT) mice (B) were stimulated for the times indicated with ADP-heptose (ADP-H) or IL-1β (A) and ADP-H or R848 (B). (C) Parental, ALPK1 KO and TIFA KO HEK293 cells were stimulated for the times indicated with ADP-H, (D) ALPK1 KO HEK293 cells were transfected with empty vector (-), FLAG-ALPK1 (WT) or FLAG-ALPK1[K1067M] (K1067M) and 48 h later were stimulated for 20 min with ADP-H. (A–D) Cell extracts were analysed directly by SDS–PAGE and immunoblotting was performed using antibodies that recognise phosphorylated (p) forms of the indicated proteins, or with antibodies recognising all forms of TIFA, ALPK1, IκBα and GAPDH. In (C,D), ALPK1 was detected after its immunoprecipitation from the extracts with an ALPK1 antibody (see Methods). The molecular mass markers needed to gauge the size of each band are shown in Supplementary Figure S7.

signalling (Supplementary Figure S2B). ADP-heptose signalling was restored by re-transfecting WT ALPK1 into ALPK1 KO cells, but not by re-transfection of the kinase-inactive ALPK1[K1067M] mutant (Figure 1D).

The expression of TAK1 and its protein kinase activity is required for ADP-heptose signalling in HEK293 cells

In HEK293 cells, IL-1β signalling requires the protein kinase TAK1 (also termed MAP3K7). TAK1 activates the MAPK kinases (MKKs) that activate p38α/p38γ and JNK1/2 and also initiates IKK activation [22,23], but the MAP3K that mediates ADP-heptose signalling is unknown. We found that ADP-heptose induced the phosphorylation of TAK1 at Thr187 in the activation loop (Figure 1A) and therefore investigated whether TAK1 was the MAP3K that drives this pathway. ADP-heptose signalling was abolished in TAK1 KO HEK293 cells (Figure 2A) and could be restored by the re-expression of WT TAK1 but not by the kinase-inactive TAK1
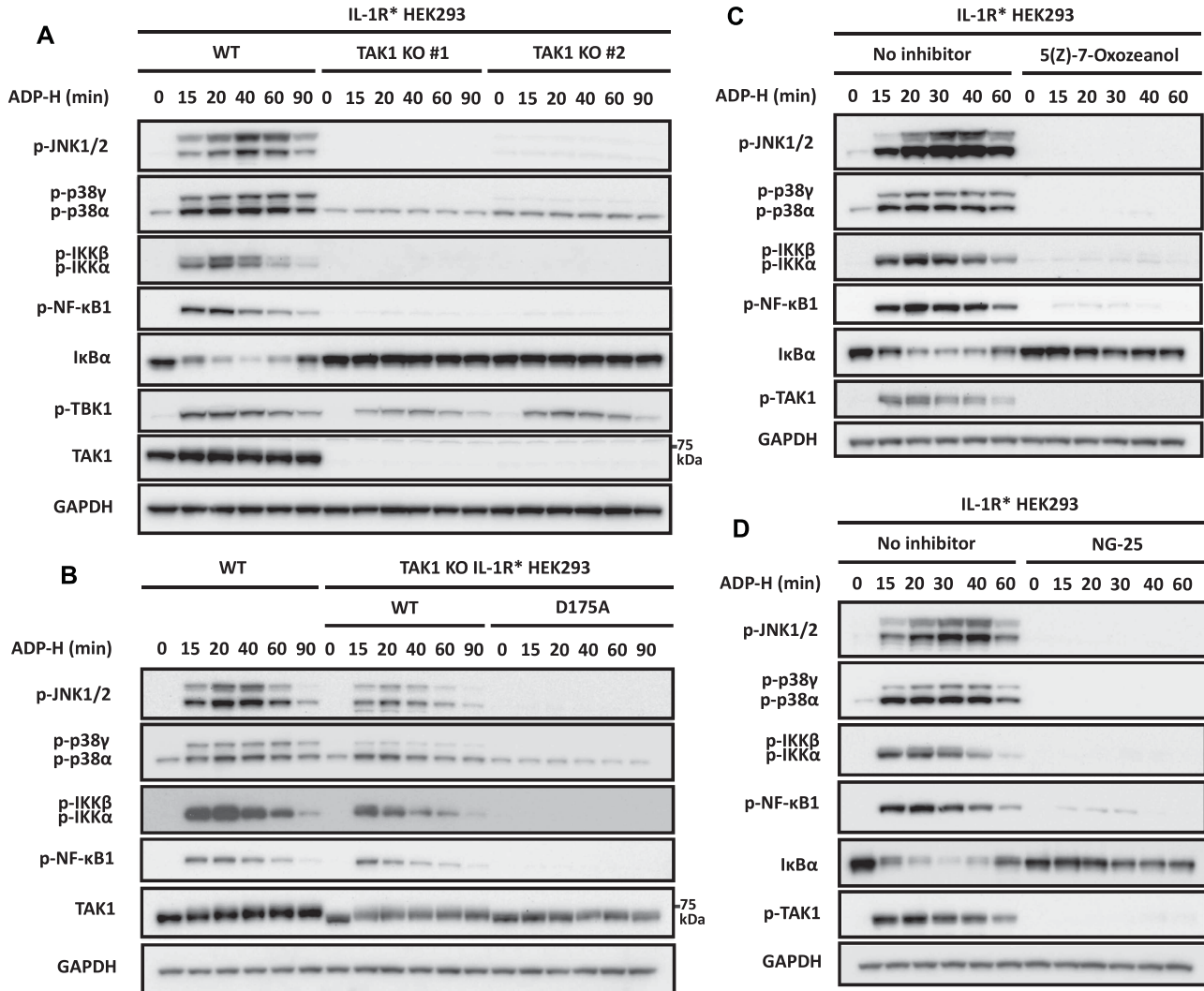
Figure 2. TAK1 and its protein kinase activity are required for ADP-heptose to activate MAP kinases and the canonical IKK complex.
(**A**) The parental and two independently isolated clones of TAK1 KO IL-1R* HEK293 cells were stimulated for the times indicated with ADP-heptose
(ADP-H). (**B**) As in (**A**), except that WT TAK1 or the kinase-inactive TAK1[D175A] mutant were stably expressed in TAK1 KO cells under a
doxycycline-inducible promoter and expression induced for 16 h with 50 ng/ml doxycycline, prior to stimulation with ADP-H for the times indicated.
(**C,D**) IL-1R* HEK293 cells were treated for 1 h with 2 μM (5Z)-7-oxozeaenol (**C**) or 5 μM NG25 (**D**) and then stimulated with ADP-H for the times
indicated. (**A–C**) Cell extracts were subjected to SDS–PAGE and immunoblotted with the antibodies indicated. The molecular mass markers needed
to gauge the size of each band are shown in Supplementary Figure S7.

[D175A] mutant (Figure 2B). ADP-heptose signalling was also abolished by two relatively specific, structurally
unrelated inhibitors of TAK1, 5(Z)-7-oxozeanol [24] (Figure 2C) and NG25 [25] (Figure 2D) whose off-target
effects on other protein kinases do not overlap (https://www.kinase-screen.mrc.ac.uk/kinase-inhibitors). We also
found that both TAK1 inhibitors suppressed the phosphorylation of TAK1 at Thr187 (Figure 2C,D), implying
that TAK1 is being activated by autophosphorylation.

ADP-heptose stimulates the formation of Lys63-linked and Met1-linked ubiquitin chains

In the IL-1β signalling pathway TAK1 is activated by the formation of Lys63-linked ubiquitin (K63-Ub) chains,
which bind to the TAB2 and TAB3 regulatory components of the TAK1 complex, inducing a conformational

change that permits the autoactivation of TAK1 [22,26,27]. IL-1β signalling also stimulates the formation of Met1-linked ubiquitin (M1-Ub) chains in HEK293 cells, which are catalysed by the HOIP component of the linear ubiquitin assembly complex (LUBAC) [28,29]. The M1-Ub chains bind to the NEMO (NF-κB essential modifier) subunit of the canonical IKK complex [30,31], inducing a conformational change that enables TAK1 to initiate the activation of IKKβ [22]. Here, we found that ADP-heptose also stimulates the formation of K63-Ub and M1-Ub chains in HEK293 cells (Supplementary Figure S3A) or mouse BMDM (Supplementary Figure S3B), although the extent of ubiquitylation is lower than in IL-1β-stimulated HEK293 cells (Supplementary Figure S3A) or R848-stimulated mouse BMDM (Supplementary Figure S3B). Consistent with a key role for K63-Ub chains in the activation of TAK1, we found that ADP-heptose signalling was suppressed in TAB2/3 double KO HEK293 cells, even allowing for the decreased expression of TAK1 in these cells (Supplementary Figure S3C). In addition, phosphorylation of NF-κB1 was reduced in mouse embryonic fibroblasts (MEFs) from mice expressing the catalytically inactive HOIP mutant, HOIP[C879S] (Supplementary Figure S3D) and obliterated in MEFs from mice expressing a ubiquitin-binding defective mutant of NEMO, NEMO[D311N] (Supplementary Figure S3E), without affecting the phosphorylation of p38α (Supplementary Figure S3D,E).

TRAF6 is required for ADP-heptose signalling, but its E3 ligase activity is not

The ADP-heptose-dependent phosphorylation (activation) of JNK1/2 and IKK was abolished in TRAF6 KO HEK293 cells (Figure 3A) and in primary TRAF6 KO macrophages derived from foetal liver cells (Figure 3B). The phosphorylation of p38γ MAPK (which is not expressed in BMDM) was also abolished in HEK293 cells (Figure 3A). These results are consistent with a previous report that the expression of TRAF6 is required for ADP-heptose signalling [5]. However, trace residual ADP-heptose-dependent phosphorylation of p38α MAPK was still detectable in TRAF6 KO cells (Figure 3A,B).

Interestingly, ADP-heptose signalling could be restored to TRAF6 KO HEK293 cells by the re-expression of WT TRAF6, and substantially restored by the re-expression of the E3 ligase-inactive TRAF6[L74H] mutant or the TRAF6[120–522] mutant in which the RING (really interesting new gene) domain of TRAF6, which carries the E3 ligase activity, is deleted (Figure 3C). The ADP-heptose-stimulated activation of MAPKs was similar in primary BMDM from knock-in mice expressing the TRAF6[L74H] mutant and in WT mice (Figure 3D). The ADP-heptose-stimulated phosphorylation of IKKα/β was partially reduced in BMDM from TRAF6[L74H] mice, but the rate of degradation of IκBα and its rate of resynthesis, as well as the phosphorylation of NF-κB1, were similar to BMDM from WT mice (Figure 3D), indicating that the activation of IKKα/β was sufficient to activate NF-κB near maximally. In contrast, R848 signalling was reduced partially in BMDM from TRAF6[L74H] mice (Figure 3E).

We have reported previously that TRAF6[L74H] and WT TRAF6 are expressed at similar levels in macrophages [23]. Taken together these experiments establish that although TRAF6 is required for ADP-heptose signalling, its E3 ligase activity is not.

The TRAF6 E3 ligase activity is also not essential for IL-1β signalling in HEK293 cells or TLR signalling in primary BMDM [23]. This is because the Pellino E3 ligases (Pellino 1 and Pellino 2), which are activated by an IRAK1-catalysed phosphorylation mechanism during IL-1β signalling, also form K63-Ub chains [32–34] and operate redundantly with TRAF6 to generate the K63-Ub chains required for the activation of TAK1 [23,35]. We, therefore, wondered whether the K63-Ub chains required for the ADP-heptose-stimulated activation of TAK1 might also be formed by TRAF6 and another E3 ligase, explaining why the E3 ligase activity of TRAF6 was not essential for ADP-heptose signalling.

Identification of proteins that immunoprecipitate with TRAF6 in ADP-heptose-stimulated cells

To investigate the identity of the putative E3 ligase, we studied the composition of TRAF6 complexes formed after stimulation for 20 min with ADP-heptose, the time at which IKK activation was maximal. We stably expressed FLAG-TRAF6 in TRAF6 KO HEK293 cells, captured TRAF6 by immunoprecipitation with a FLAG antibody, and released the TRAF6-binding proteins by incubation with FLAG peptide. These proteins were then identified by mass spectrometry (MS) using tandem mass tag (TMT) quantification. The Volcano plot (Figure 4A) revealed that major proteins captured in an ADP-heptose-dependent manner included TIFA, the four components of the TAK1 complex (TAB1, TAB2, TAB3 and TAK1), IKKα and IKKβ, the three
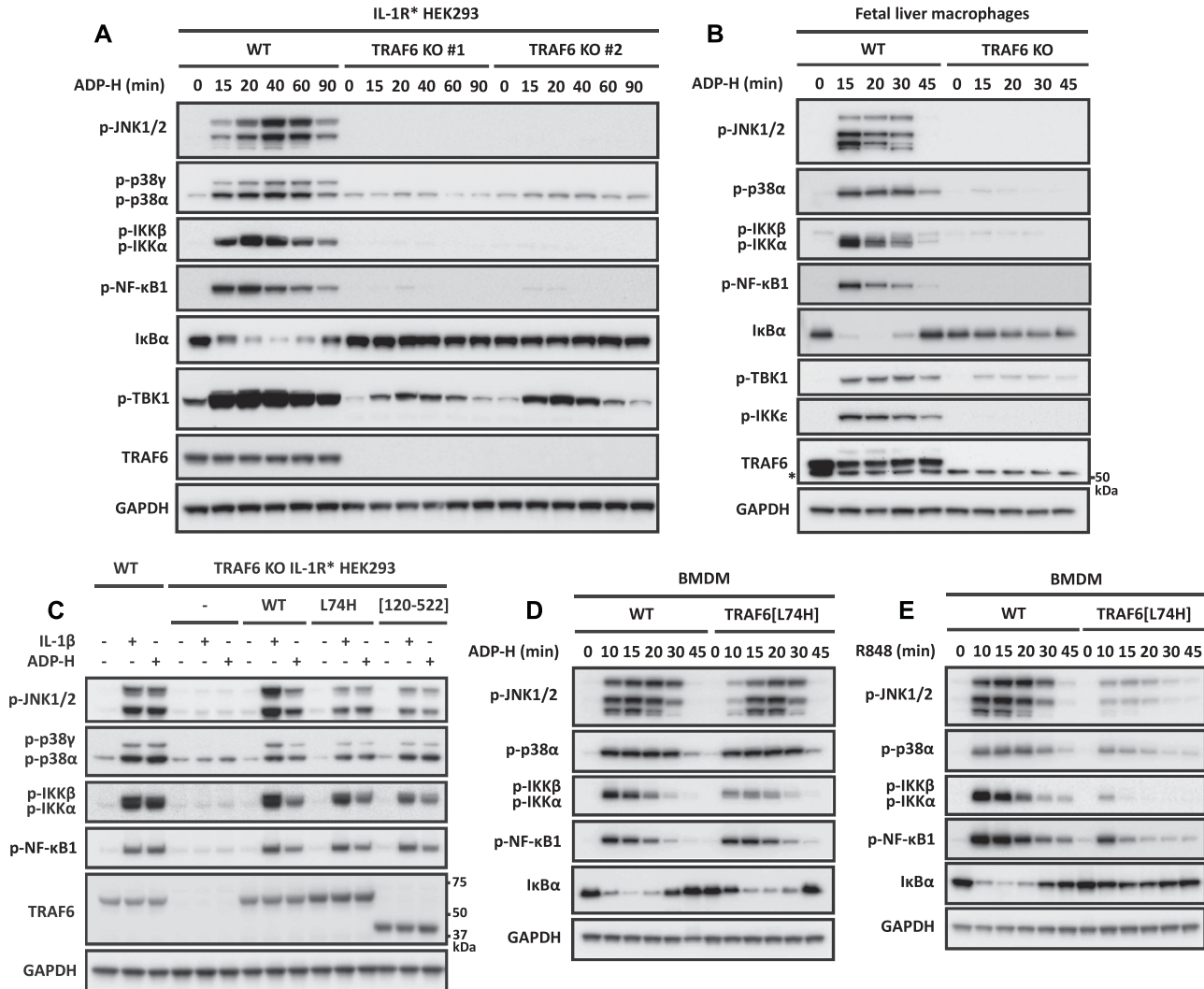
Figure 3. TRAF6 is required for ADP-heptose signalling in HEK293 cells and primary macrophages, but its E3 ligase activity is not.
(**A**) Parental and two independently isolated clones of TRAF6 KO IL-1R* HEK293 cells were stimulated for the times indicated with ADP-heptose (ADP-H). (**B**), As in (**A**), except that WT TRAF6, TRAF6[L74H] or TRAF6[120–522] were stably expressed in TRAF6 KO IL-1R* HEK293 cells under a constitutive promoter and stimulated for 20 min with ADP-H or IL-1β. (**C**) Foetal liver macrophages from wild-type (WT) and TRAF6 KO embryos were stimulated for the times indicated with ADP-H. (**D,E**) BMDM from WT and TRAF6[L74H] mice were stimulated for the times indicated with ADP-H (**D**) or R848 (**E**). (**A–E**) Cell extracts were subjected SDS–PAGE and immunoblotted using the indicated antibodies. An asterisk indicates protein(s) recognised non-specifically by an antibody. The molecular mass markers needed to gauge the size of each band are shown in Supplementary Figure S7.

components of LUBAC (Sharpin, HOIL-1 and HOIP) and the HOIP-interacting protein WRNIP1 that contains a ubiquitin-binding zinc finger domain and a Glu-Glu-His-Tyr-Asn motif that may mediate binding to the PUB domain of HOIP [36]. They also included A20 and ABIN1 (A20-binding inhibitor of NF-κB), two proteins known to restrict IL-1β and TLR signalling by binding to M1-Ub and K63-Ub chains [35]. Other proteins that were captured included TRAF2, its known binding partner c-IAP1, and the c-IAP1-binding proteins SMAC and HtrA2/Omi. SMAC and HtrA2 are mitochondrial proteins that bind to c-IAP1 only when mitochondria are disrupted [37], which most likely occurred in the present study during cell lysis, as a result of the inclusion of the detergent Triton X-100 in the cell lysis buffer.

TRAF2 was originally found to bind to TIFA in a mammalian two-hybrid screen [6] and in AGS cells infected with *H. pylori* [16], and c-IAP1 is an E3 ligase. We, therefore, wondered whether TRAF2 might recruit
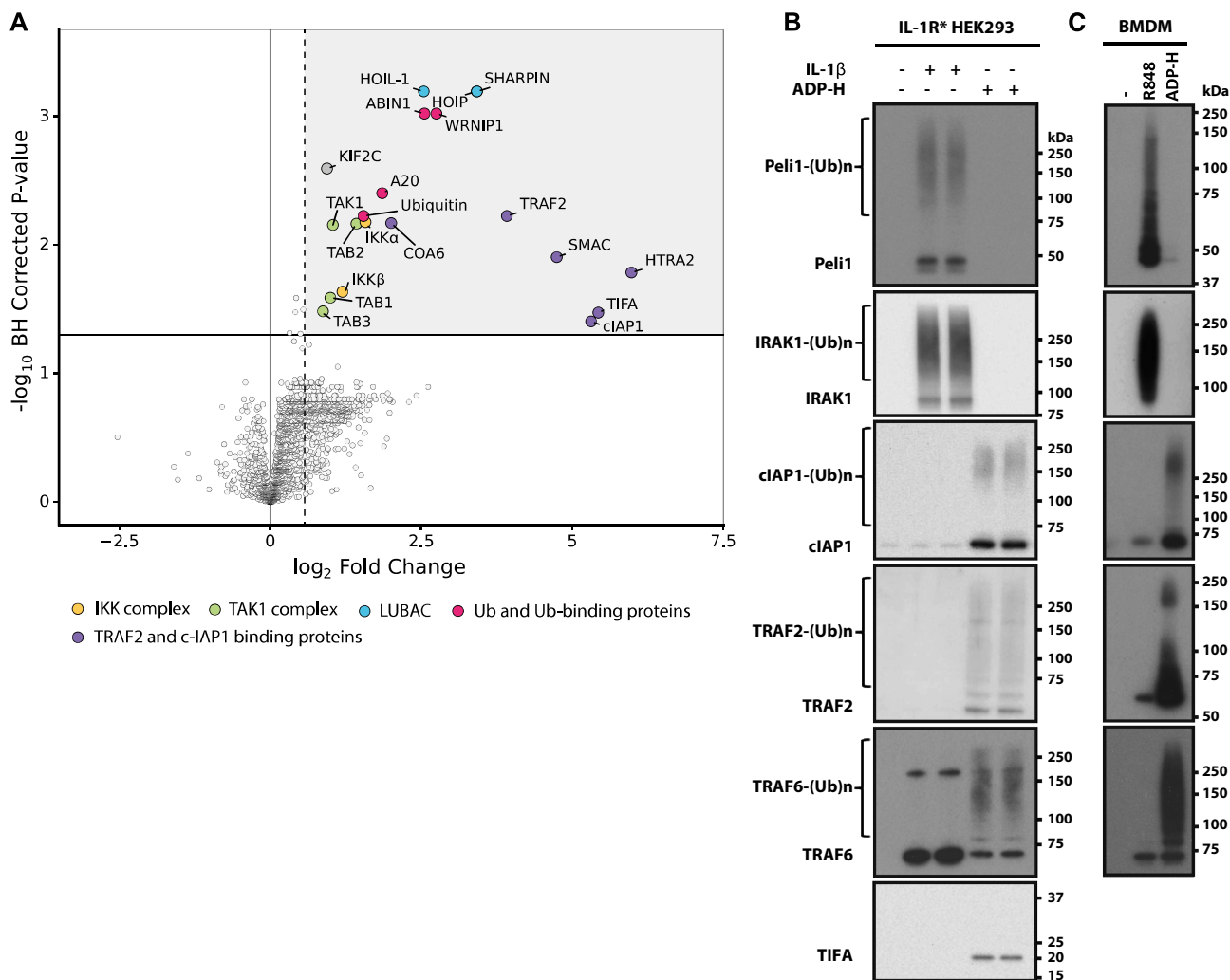
Figure 4. Proteins enriched in TRAF6 immunoprecipitates in ADP-heptose-stimulated HEK293 cells.

(**A**) IL-1R* HEK293 cells were stimulated for 20 min with ADP-heptose (ADP-H) and proteins in cell extracts immunoprecipitated with FLAG-TRAF6 were analysed by TMT mass spectrometry. The figure shows a volcano plot identifying the proteins where enrichment attained statistical significance and where the fold increase was >1.5-fold. (**B**) HEK293 cells were stimulated for 15 min with ADP-H or IL-1β and the proteins shown that were captured from the cell extracts on Halo-NEMO beads were identified by SDS–PAGE followed by immunoblotting with the antibodies indicated. (**C**) WT BMDM were stimulated for 15 min with ADP-H or R848 and analysed with the same antibodies used in (**B**), except for c-IAP1, where a mouse-specific antibody was used (see Methods). Ubiquitylated forms of proteins are indicated by (Ub)$_n$.

c-IAP1 to TIFA during ADP-heptose signalling to produce K63-Ub chains required for the activation of TAK1. To investigate this hypothesis, we used Halo-NEMO beads to capture K63- and M1-Ub chains from HEK293 cell extracts, as well as the proteins to which they are attached covalently and non-covalently [23,38]. We found that Halo-NEMO beads captured ubiquitylated forms of c-IAP1, TRAF2 and TRAF6 in an ADP-heptose-dependent manner but did not capture IRAK1 or Pellino 1 (Figure 4B). In contrast, the Halo-NEMO beads captured ubiquitylated forms of Pellino 1 and IRAK1 in an IL-1β-dependent manner but did not capture c-IAP1 or TRAF2 (Figure 4B). The c-IAP2 isoform was not detected in the Halo-NEMO pull-downs because it is not expressed in HEK293 cells (Supplementary Figure S4). The Halo-NEMO beads also captured ubiquitylated c-IAP1 and TRAF2 from the extracts of ADP-heptose stimulated mouse BMDM, but not Pellino 1 or IRAK1; conversely, Halo-NEMO beads captured ubiquitylated Pellino 1 and IRAK1 from the extracts of R848-stimulated mouse BMDM but not c-IAP1 or TRAF2 (Figure 4C). TRAF6 was also captured

from the extracts of IL-1β-stimulated HEK293 cells (Figure 4B) and R848-stimulated BMDM (Figure 4C) but, in contrast with ADP-heptose-stimulated cells, it was not ubiquitylated and was presumably captured by Halo-NEMO beads because of its interaction with ubiquitylated IRAK1. TIFA was also captured by Halo-NEMO beads from the extracts of ADP-heptose-stimulated HEK293 cells but was not ubiquitylated (Figure 4B). This could not be confirmed in mouse BMDM because the TIFA antibody only recognises the human and not the mouse protein.

Taken together, these observations indicated that ADP-heptose did not induce the activation and autoubiquitylation of Pellino 1, suggesting that Pellino isoforms were unlikely to be the putative E3 ligases operating redundantly with TRAF6 during ADP-heptose signalling.

The TRAF6 and c-IAP1 E3 ligases generate the K63-Ub chains needed to propagate the ADP-heptose signal

To investigate the role of TRAF2/c-IAP1 in ADP-heptose signalling, we stably re-expressed WT TRAF6 or TRAF6[L74H] in TRAF2/TRAF6 double KO HEK293 cells. The ADP-heptose-stimulated phosphorylation of IKKα/β, NF-κB1, JNK1/2 and p38α/γ MAPK was restored to TRAF6 KO cells by the re-expression of either WT TRAF6 or TRAF6[L74H], as expected, but IKKα/β, NF-κB1 and p38γ MAPK activation could only be restored by WT TRAF6 in TRAF2/TRAF6 double KO cells (Figure 5A). However, trace phosphorylation of JNK1/2 and some phosphorylation of p38α MAPK was restored to TRAF2/TRAF6 double KO cells by the re-expression of TRAF6[L74H] but was only significant after 30–40 min. The molecular basis for this slow activation is unclear but one speculation is that it may be driven by the TRAF5 present in these cells.

Since TRAF2 appears to be an inactive 'pseudo' E3 ligase [39], these results were consistent with the notion that a key role of TRAF2 is to recruit c-IAP1 into the TIFA signalling complex, where it acts redundantly with TRAF6 to produce the K63-Ub chains required to activate TAK1. We tested this hypothesis by studying the effect of the SMAC mimetic BV-6 [40]. SMAC mimetics are small chemical entities that bind to IAP family members, inducing their autoubiquitylation and proteasomal destruction [41]. Incubation of HEK293 cells with BV-6 greatly reduced the expression of c-IAP1, as expected, and greatly reduced ADP-heptose signalling in TRAF6 KO cells reconstituted with TRAF6[L74H] (Figure 5B). The residual cIAP1 expression may explain why signalling was not completely abolished.

Taken together, these results support the conclusion that c-IAP1 is the E3 ligase that operates redundantly with TRAF6 to generate the K63-Ub chains required to activate TAK1 and hence the activation of JNK1/2 and IKKα/β and the phosphorylation of the IKKβ substrate NF-κB1 during ADP-heptose signalling in HEK293 cells.

The effects of TRAF2/c-IAP1 are not mediated by the non-canonical NF-κB pathway

It is well established that TRAF2-cIAP1/2 complexes are components of the non-canonical NF-κB pathway that induces the expression of NF-κB-inducing kinase (NIK) [42]. It has also been reported that ADP-heptose activates the non-canonical NF-κB pathway in AGS cells [43], and we confirmed this result in HT-1080 cells (Supplementary Figure S5B). However, the ADP-heptose induced expression of NIK was only detected after 2 h, much later than the degradation of IκBα, which was complete by 20 min. Moreover, even in HT-1080 cells, the ADP-heptose-stimulated appearance of NIK was much weaker than that induced by the TNF superfamily member TWEAK (TNF-like weak inducer of apoptosis) (Supplementary Figure S5B). More importantly, we were unable to detect any appearance of NIK in HEK293 cells after stimulation with ADP-heptose for up to 8 h (Supplementary Figure S5A), indicating that ADP-heptose does not activate the non-canonical NF-κB pathway in HEK293 cells. The rapid effects of TRAF2/c-IAP1 on ADP-heptose signalling in HEK293 cells described in the present study are therefore independent of the non-canonical NF-κB signalling pathway.

The ADP-heptose-stimulated activation of TBK1 is mediated by TRAF6 and TRAF2

The protein kinase TANK-binding kinase-1 (TBK1) is an IKK-related kinase that is converted from an inactive to an active form by phosphorylation at Ser172 [44]. In the present study we found that the phosphorylation
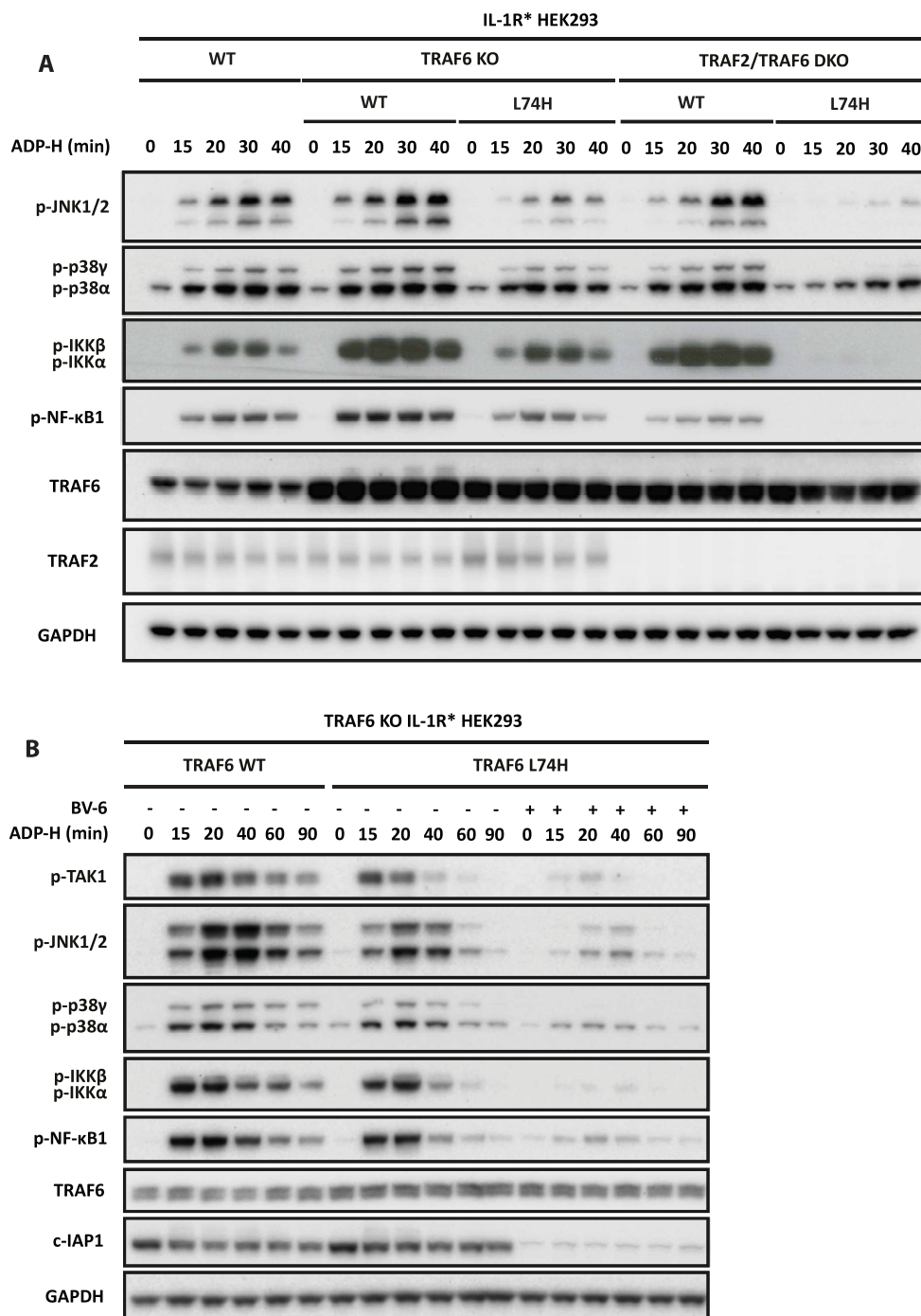
Figure 5. The TRAF6 and TRAF2/c-IAP1 operate redundantly to generate the ubiquitin chains required for ADP-heptose signalling.

(**A**) Parental, TRAF6 KO or TRAF2/6 double KO IL-1R* HEK293 cells in which WT TRAF6 or TRAF6[L74H] had been stably re-expressed under a constitutive promoter were stimulated for the times indicated with ADP-H. (**B**) TRAF6 KO IL-1R* HEK293 cells in which WT TRAF6 or TRAF6[L74H] had been stably re-expressed as in (**A**) were treated for 5 h with 5 μM BV-6 prior to stimulation for the indicated times with ADP-H. (**A,B**) The cell extracts were subjected to SDS–PAGE and immunoblotting was performed with the antibodies indicated. The molecular mass markers needed to gauge the size of each band are shown in Supplementary Figure S7.

(activation) of TBK1 was induced by ADP-heptose in HEK293 cells (Figure 1A) and BMDM (Figure 1B) but not in ALPK1 or TIFA KO HEK293 cells (Figure 1C). The ADP-heptose-stimulated phosphorylation of TBK1 was unaffected in TAK1 KO cells (Figure 2A), reduced in TRAF6 KO cells (Figure 3A) and abolished in TRAF2/TRAF6 double KO HEK293 cells (Supplementary Figure S6). We did not study the regulation of IKKε, the other IKK-related kinase, because its expression was extremely low in HEK293 cells (Supplementary Figure S4). However, we did detect the phosphorylation of IKKε in BMDM (Figure 1B), which was disrupted in TRAF6 KO foetal liver macrophages (Figure 3B). The role of TBK1 in this pathway is considered further in the discussion.

ALPK1 phosphorylates TIFA at Thr9 and Thr177

The mutation of Thr9 to Ala was shown to abolish TIFA oligomerisation in overexpression studies before the ADP-heptose signalling pathway was discovered [12]. Later, the replacement of TIFA by the TIFA[T9A] mutant was found to abolish ADP-heptose-stimulated NF-κB-dependent gene transcription and IL-8 transcript formation [5]. These experiments suggested that the phosphorylation of TIFA at Thr9 was required for ADP-heptose signalling but the direct phosphorylation of TIFA at Thr9 by ALPK1 *in vitro* has never been demonstrated. Therefore, the possibility that ALPK1 phosphorylates and activates another protein kinase, which then phosphorylates TIFA at Thr9, has also not been excluded.

We re-expressed WT and mutant forms of FLAG-TIFA in TIFA KO HEK293 cells. ADP-heptose induced the activation of JNK and IKK in cells re-expressing WT FLAG-TIFA, but not in cells expressing TIFA[T9A], as expected (Figure 6A). More surprisingly, ADP-heptose failed to induce signalling in cells expressing the TIFA[T9S] mutant, or in cells expressing the TIFA [T9D] or TIFA[T9E] mutants in which a negative charge was introduced to try to mimic the effect of phosphorylation (Figure 6A). Consistent with these findings, ADP-heptose failed to induce the binding of TRAF6 or TRAF2 to TIFA in cells expressing TIFA[T9A], TIFA [T9S], TIFA [T9D] or TIFA[T9E] (Figure 6B). We, therefore, studied the phosphorylation of TIFA by ALPK1 *in vitro* using purified proteins and Mg-[γ^{32}P]ATP.

FLAG-tagged WT ALPK1 phosphorylated itself and purified GST-TIFA *in vitro* but no incorporation of ^{32}P-radioactivity into these proteins occurred when WT ALPK1 was replaced by the kinase-inactive ALPK1 [K1067M] mutant (Figure 6C). The phosphorylation of TIFA was reduced by 64% when GST-TIFA was replaced by GST-TIFA[T9A] (Figure 6D,E), suggesting that Thr9 was not the only site of phosphorylation. Interestingly, ALPK1 phosphorylated GST-TIFA[T9S] as efficiently as WT TIFA (Figure 6D,E), indicating that TIFA phosphorylated at Ser9 is unable to interact with the FHA domain of TIFA and hence cannot induce the oligomerisation of TIFA that is required to initiate signalling.

Inspection of the amino acid sequence of human TIFA revealed that the putative tryptic phosphopeptide containing Thr9 would be very large and hydrophobic (and therefore probably insoluble) in 0.1% (v/v) trifluoracetic acid, the solvent used routinely to separate peptides by HPLC. In an initial experiment using unlabelled ATP, TIFA phosphorylated by ALPK1 was digested with chymotrypsin and subjected to MS. A phosphopeptide was detected comprising amino acid residues 5–21 of TIFA phosphorylated at Thr9 (EDADT*EETVTCLQMTVY, where T* is Thr9). A further peptide was detected comprising residues 2–16 of TIFA phosphorylated at Thr9, which was preceded by the sequence Gly-Ser (GSTSFEDADT*EETVTCL, where T* is Thr9). The Gly-Ser sequence is derived from the linker region (GPLGS) between GST and TIFA that remains attached to TIFA after cleavage of GST-TIFA with PreScission Protease. A third phosphopeptide was identified comprising the C-terminal peptide of TIFA, residues 167–184 (SLCSSQSSSPTEMDENES), but the site of phosphorylation could not be identified in this experiment (Figure 6F).

We next phosphorylated TIFA using Mg-γ^{32}P-labelled ATP and subjected the chymotryptic digest to chromatography on a C$_{18}$ column, which resolved five major ^{32}P peptides C1–C5 (Figure 7A). MS indicated that peptides C1, C2 and C4 were all phosphorylated at Thr9 (Figure 7D). Solid phase sequencing of peptides C2 and C4 released ^{32}P-radioactivity after the 7th and 13th cycles of Edman degradation, respectively, confirming that Thr9 was the site of phosphorylation (Figure 7B,C). The minor ^{32}P-peptides C3 and C5 could not be identified by MS.

To identify the phosphorylated amino acid residue in the C-terminal peptide of TIFA, we phosphorylated TIFA[T9A] with ALPK1 and subjected it to more prolonged digestion with a 2-fold higher concentration of chymotrypsin. HPLC analysis of the digest revealed a major peptide, T177 (Figure 7E), with a molecular mass corresponding to amino acid residues 167–184 of TIFA (SLCSSQSSSPTEMDENES) plus one phosphate group
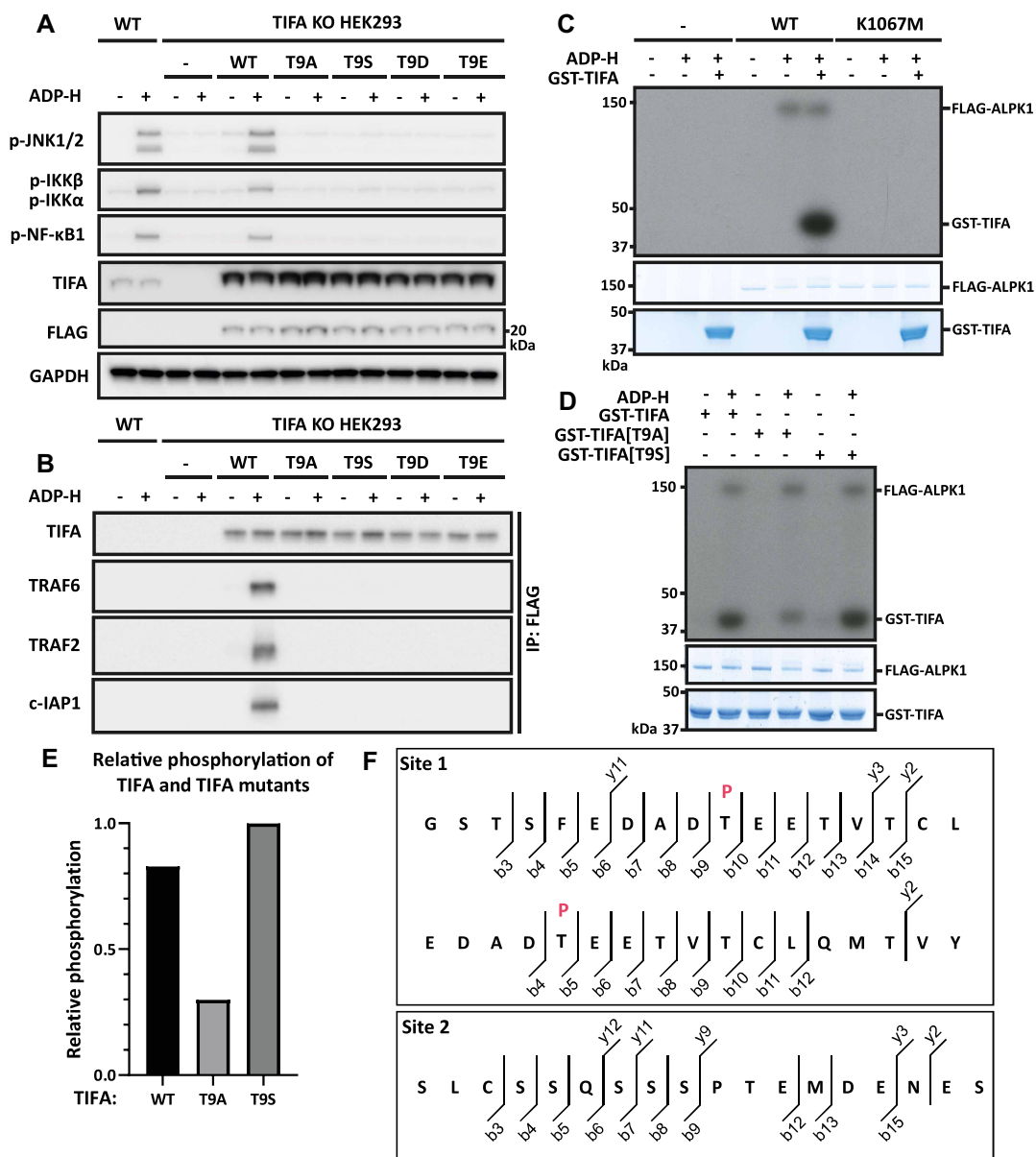
Figure 6. ALPK1 phosphorylates TIFA directly at Thr9 *in vitro*.

(A) TIFA KO HEK293 cells were re-transfected with 500 ng of DNA plasmid encoding FLAG-TIFA or the indicated FLAG-TIFA mutants. After 24 h, the cells were stimulated for 20 min with ADP-heptose (ADP-H) and cell extracts subjected to SDS-PAGE and immunoblotting with the antibodies indicated. **(B)** Cell extracts (1.0 mg protein) from **(A)** were immunoprecipitated with anti-FLAG, then subjected to SDS-PAGE and immunoblotting. **(C-E)** ALPK1 KO HEK293 cells were re-transfected with 2.5 mg plasmid DNA encoding empty vector (-), FLAG-ALPK1 and FLAG-ALPK1[K1067M] as indicated. After 48 h, ALPK1 was immunoprecipitated from the cell extracts with FLAG antibody and phosphorylation performed for 20 min with 8 μM GST-TIFA or GST-TIFA mutants, 10 mM magnesium acetate and 0.1 mM [γ-^{32}P]ATP (1000 cpm/pmol) with or without or without 100 nM ADP-H. The ^{32}P-radioactivity incorporated was visualised by autoradiography **(C, D)** and quantitated by Cerenkov counting **(E)**. In **(D, E)**, phosphorylation of WT TIFA was compared with TIFA[T9A] in three experiments, but phosphorylation of WT TIFA with TIFA [T9S] was compared once. **(F)** FLAG-ALPK1 was immunoprecipitated from the cell extracts as in **(C-E)** and phosphorylation performed for 20 min with 8 μM of TIFA and 0.1 mM unlabelled ATP with or without 100 nM ADP-H. The reactions were stopped by denaturation in SDS, separated by SDS-PAGE and the band corresponding to TIFA was excised, digested for 24 h with chymotrypsin and the resulting peptides identified by mass spectrometry. The phospho-peptides identified are shown along with their b- and y- ions. Where localisation confidence was > 80%, the phosphorylated residue has been indicated in red.

(Figure 7G). Solid phase sequence analysis revealed that ^{32}P-radioactivity was released from the peptide after the 11th cycle of Edman degradation (Figure 7F), identifying Thr177 as the site of phosphorylation.

Evidence that phosphorylation of Thr177 in the TRAF6-binding motif suppresses binding to TRAF6 but not TRAF2

Interestingly, Thr177 lies within a TRAF6-binding motif Pro-Xaa-Glu [45], where Xaa can be any amino acid residue. It has been reported that the TIFA[E178A] mutant, which disrupts the TRAF6-binding motif, fails to induce the oligomerisation and activation of TRAF6 in a cell-free system [9], and fails to stimulate NF-κB-dependent luciferase reporter gene expression when overexpressed in TIFA KO HEK293 cells [5]. Consistent with these findings, we found that ADP-heptose also failed to induce MAPK and IKK phosphorylation (Figure 8A) or interaction with TRAF6 (Figure 8B) when the TIFA[E178A] mutant was re-expressed in TIFA KO cells, in contrast with WT TIFA. However, the ADP-heptose-dependent interaction of TIFA[E178A] with TRAF2 and c-IAP1 was unaffected (Figure 8B). These findings imply that TRAF2 and TRAF6 bind to distinct sites on TIFA, and that TRAF2 is not captured by TIFA because it heterodimerises with TRAF6 [46].

The TIFA[T177A] mutant did not impair ADP-heptose stimulated activation of MAPKs and IKKα/β (Figure 8C), nor the interaction of TIFA with TRAF6, TRAF2 and c-IAP1 (Figure 8D). In contrast, the phospho-mimetic TIFA[T177D] mutant greatly reduced ADP-heptose-stimulated MAPK and IKK phosphorylation (Figure 8C) and interaction with TRAF6 (Figure 8D), but the interaction with TRAF2 and c-IAP1 was unaffected (Figure 8D).

Discussion

In this paper, we have made several findings that have advanced understanding of the ADP-heptose signalling network. First, we have established that the expression and activity of TAK1 are required for the ADP-heptose-dependent activation of the p38 MAP kinases, JNK1/2 and the canonical IKK complex. Second, the K63-linked ubiquitin chains required to activate TAK1 are formed by both the TRAF6 and c-IAP1 E3 ligases, explaining why the E3 ligase activity of TRAF6 is not essential for the operation of the pathway. Third, we have found that ADP-heptose triggers the formation of M1-linked ubiquitin chains, which are known to facilitate the activation of the canonical IKK complex.

Why the expression of TRAF6 is essential for the activation of MAP kinases and the canonical IKK complex, even though its E3 ligase activity is not, is unclear, but we speculate that the interaction of TRAF6 with TAK1, as well as the binding of K63-Ub chains to the TAB2/3 subunits of the TAK1 complex [47], may be needed for the activation of TAK1.

Although TRAF6 ubiquitylation was originally believed to be a key event in MyD88 signalling it was later reported that a TRAF6 mutant in which every Lys was mutated to Arg restored IL-1 signalling to TRAF6 KO fibroblasts [48]. Curiously, we now find that endogenous TRAF6 does not undergo ubiquitylation after stimulation with IL-1β in HEK293 cells or by R848 in BMDM. However, it does become ubiquitylated in response to stimulation with ADP-heptose. It will now be interesting to investigate whether TRAF6 ubiquitylation has an important role in ADP-heptose signalling.

The formation of M1-linked ubiquitin chains is catalysed by the HOIP component of LUBAC, which was recruited to the TIFA–TRAF6–TRAF2/c-IAP1 signalling complex together with its binding partner WRNIP1 in response to ADP-heptose (Figure 4A). An important role for M1-Ub chains in ADP-heptose signalling was indicated by the reduced ADP-heptose-dependent NFκB1 phosphorylation in MEFs expressing an E3 ligase-inactive mutant of HOIP (Supplementary Figure S3D) or in MEFs expressing the NEMO[D311N] mutant that is unable to bind to M1-Ub linkages (Supplementary Figure S3E).

A fourth finding that we made is that ADP-heptose stimulates the phosphorylation of the IKK-related kinase TBK1 at Ser172, the site required for TBK1 activation [44]. The ADP-heptose-stimulated phosphorylation of TBK1 was reduced in TRAF6 KO cells (Figure 3A) but did not require the expression or activity of TAK1 (Figure 2A) and was abolished in TRAF2/6 double KO cells (Supplementary Figure S6). TRAF2, therefore, has a role in the ADP-heptose-dependent activation of TBK1 that can be mediated independently of TRAF6 and does not simply function as a modulator of TRAF6-dependent signalling. An updated schematic of the ADP-heptose signalling pathway that incorporates our findings is shown in Figure 9.

One of the physiological roles of TBK1 is to restrict the activation of the canonical IKK complex [49] by phosphorylating inhibitory sites on IKKα/β and on their regulatory subunit NEMO [50,51]. Such mechanisms
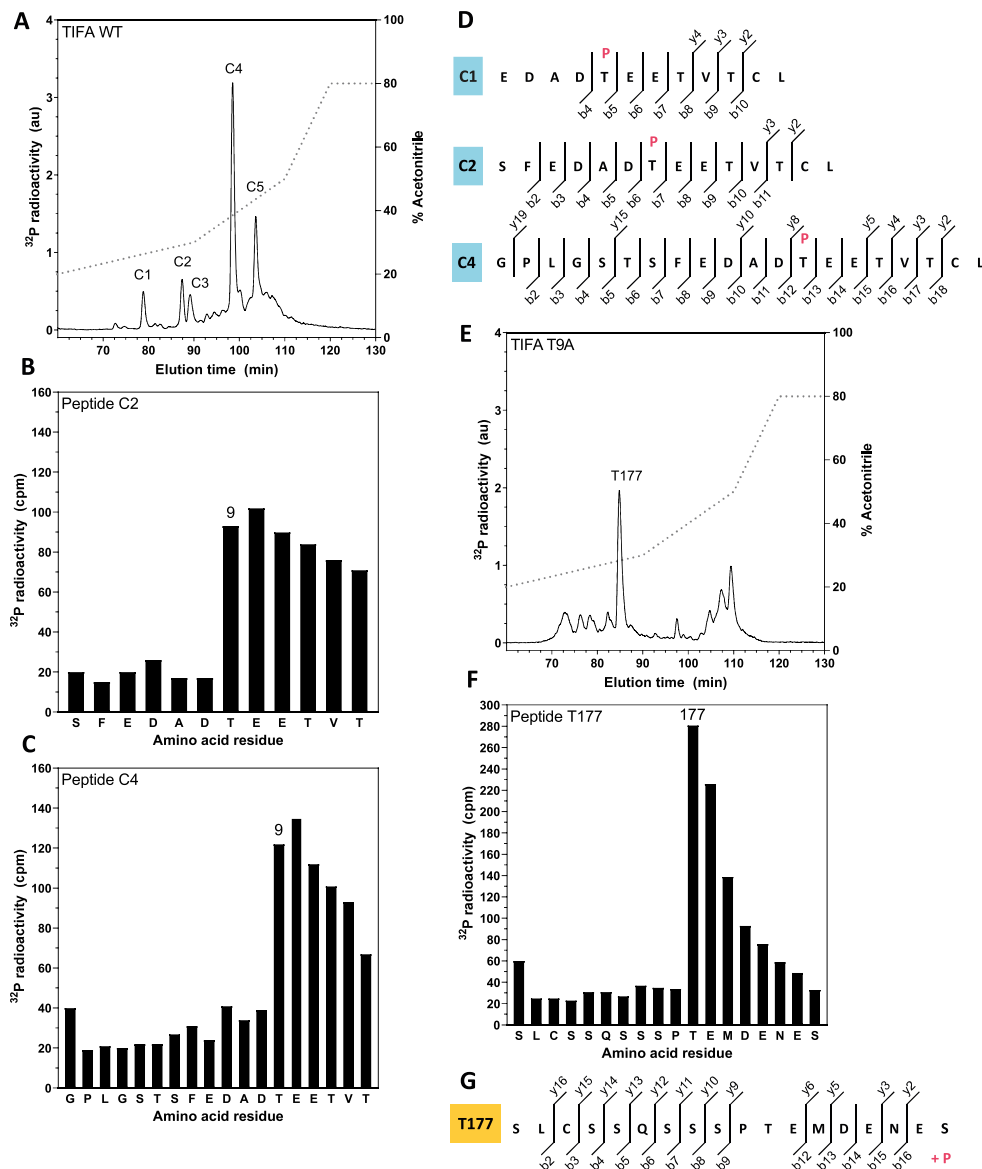
PORTLAND PRESS

Figure 7. ALPK1 phosphorylates TIFA directly at Thr177 and Thr9.
(A) ALPK1 KO HEK293 cells were re-transfected with plasmid DNA encoding FLAG-ALPK1 and FLAG-ALPK1 immunoprecipitated and used to phosphorylate TIFA as in Fig 6F except using [g^{32}P]ATP. The ^{32}P-labelled TIFA was excised, digested for 24 h with chymotrypsin and the digest separated by HPLC with on-line radioactivity detection (see Methods). The solid line indicates the ^{32}P-radioactivity and the broken line the acetonitrile gradient. **(B, C)** The peptides corresponding to C2 **(B)** and C4 **(C)** in **(A)** were subjected to solid phase sequencing and ^{32}P-radioactivity released at each cycle of Edman degradation quantitated by Cerenkov counting. **(D)** Peptides C1, C2 and C4 were subjected to mass spectrometry and the phospho-peptides detected are indicated along with their respective b- and y- ions. The site of phosphorylation is shown where localisation confidence was >90%. **(E)** As in **(A)** except that TIFA[T9A] was the substrate. **(F)** Peptide T177 from E was subjected to solid phase sequencing as in **(B, C)**. **(G)** Peptide T177 was subjected to mass spectrometry and the mass fragmentation pattern is shown.

are needed to prevent the hyperactivation of innate immune signalling pathways, which would otherwise lead to the overproduction of inflammatory mediators that cause inflammatory and autoimmune diseases. It is, therefore, noteworthy that two other negative regulators of innate immune signalling pathways, the ubiquitin-
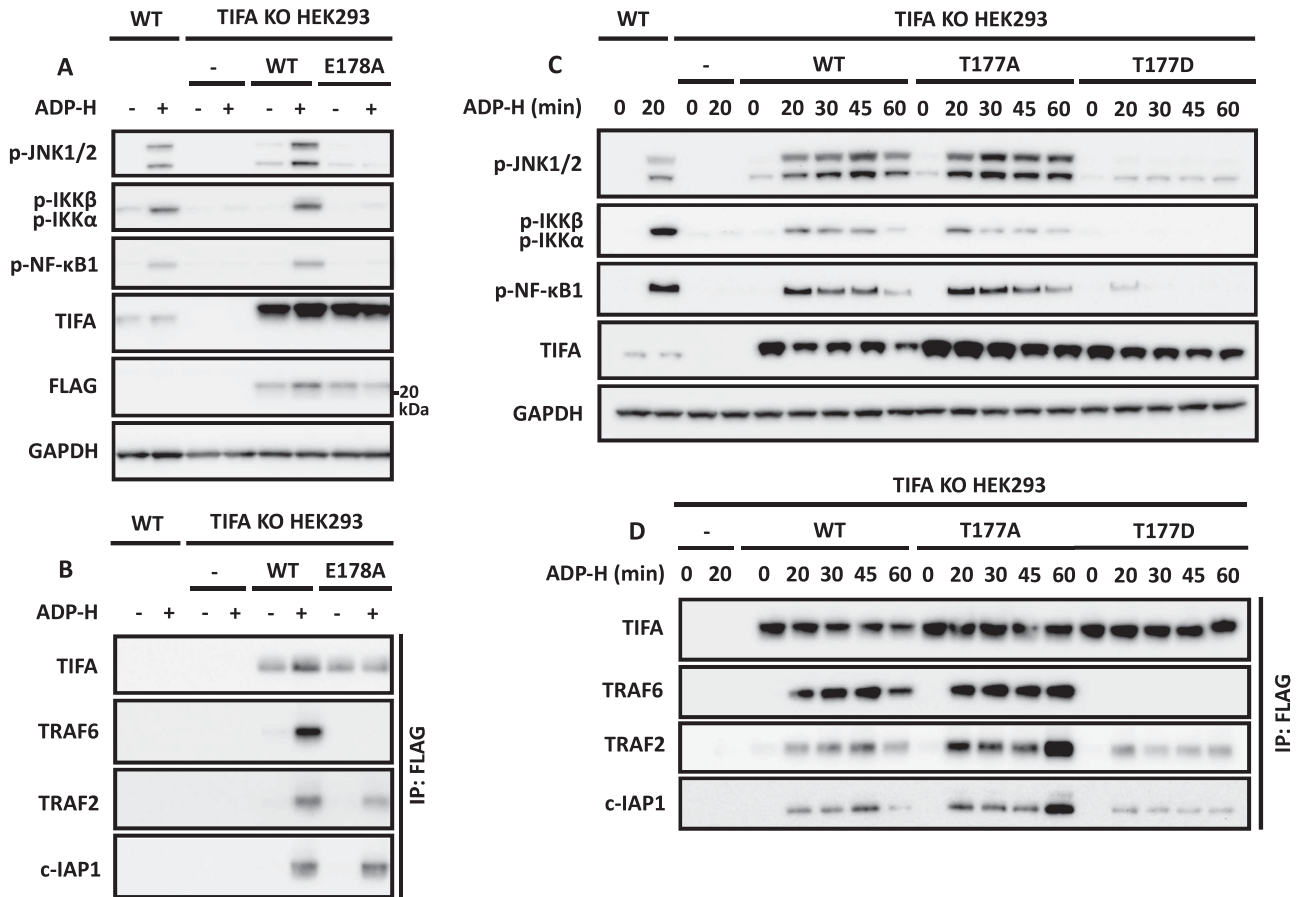
Figure 8. Mutations that disrupt the TRAF6-binding site of TIFA do not affect the interaction of TIFA with TRAF2.
(**A**) TIFA KO HEK293 cells were re-transfected with 500 ng of plasmid DNA encoding empty vector (-), FLAG-TIFA or FLAG-TIFA[E178A]. Twenty-four hours later the cells were stimulated for 20 min with ADP-H and the extracts subjected to SDS–PAGE and immunoblotting with the antibodies indicated. (**B**) Cell extracts from (**A**) were immunoprecipitated with anti-FLAG and the immunoprecipitates analysed as in (**A**). (**C**) As in (**A**), except that plasmid DNA encoding empty vector, FLAG-TIFA, FLAG-TIFA[T177A] or FLAG-TIFA[T177D] was transfected. (**D**) As in (**B**) but using extracts from (**C**). The molecular mass markers needed to gauge the size of each band are shown in Supplementary Figure S7.

binding proteins A20 and ABIN1 (reviewed [35]), were also recruited to the ADP-heptose-stimulated signalling complex (Figure 4A). The disappearance of TIFA during prolonged ADP-heptose stimulation may be an additional mechanism of negative regulation (Figure 1C).

We have also established for the first time that ALPK1 phosphorylates TIFA directly at Thr9 and identified Thr177 as a second site phosphorylated by ALPK1. Interestingly, Thr177 lies in the TRAF6-binding motif of TRAF6 (Pro-Thr-Glu) and its mutation to Asp to try and mimic the effect of phosphorylation by introducing a negative charge at this position, suppressed the binding of TRAF6 to TIFA and consequently greatly reduced the ADP-heptose-stimulated phosphorylation of MAP kinases and the canonical IKK complex (Figure 8C). The ALPK1-catalysed phosphorylation of TIFA at Thr177 may represent yet a further mechanism for restricting the strength of activation of the ADP-heptose signalling pathway. The TIFA[T177D] mutation did not affect interaction with TRAF2, indicating that the binding of TRAF2 to TIFA occurs independently of the binding of TRAF6 (Figure 8D). The TIFA[T9A] and other TIFA mutants prevent the binding of both TRAF6 and TRAF2 because they prevent the formation of TIFA oligomers, which is essential to recruit the proteins needed to propagate the ADP-heptose signal. TIFA does not possess either of the known TRAF2-binding motifs Pro/Ser/Ala/Thr-Xaa-Gln/Glu-Glu and Pro-Xaa-Gln-Xaa-Xaa-Asp [52], and it will be important to define the TRAF2-binding site in TIFA in future studies.
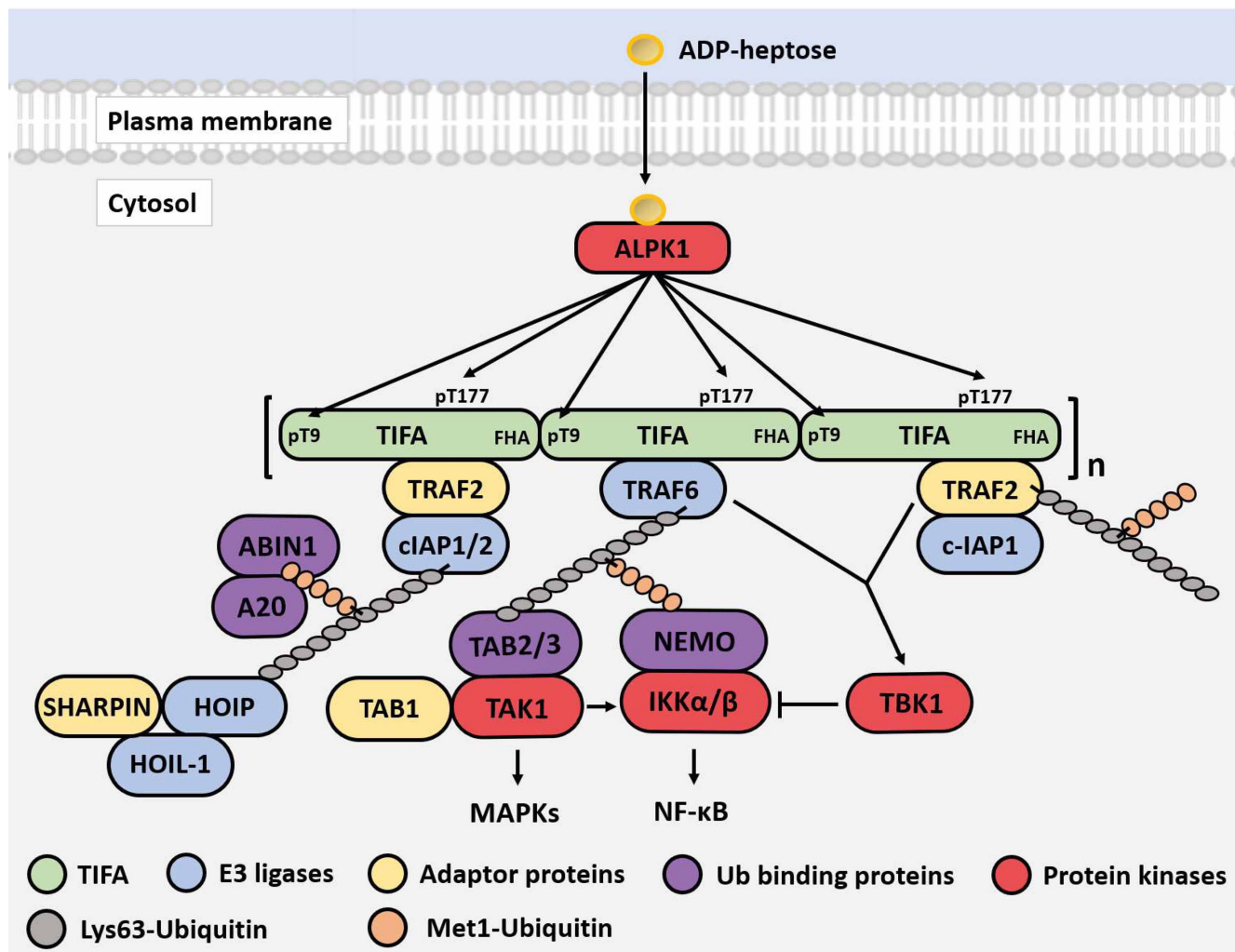
Figure 9. Schematic of the ADP-heptose signalling pathway in HEK293 cells.
ADP-heptose enters the cytosol through an unidentified transporter where it binds to an allosteric site in ALPK1 inducing activation and enabling it to phosphorylate TIFA at Thr9 and Thr177. The phosphorylated Thr9 interacts with the FHA domain of another TIFA molecule, leading to TIFA polymerisation in a head-to-tail fashion. This permits TRAF6 to interact with the TRAF6-binding motif of TIFA leading to the oligomerisation of TRAF6 and activation of its E3 ligase activity. The polymerised TIFA also recruits TRAF2 to an unknown site. The E3 ligase c-IAP1, which forms a complex with TRAF2, combines with TRAF6 to generate Lys63-linked ubiquitin oligomers that become attached covalently to TRAF6, TRAF2 and c-IAP1 and interact with the TAB2 or TAB3 components of TAK1 complexes, inducing the autoactivation of TAK1. ADP-heptose also stimulates the formation of Met1-linked ubiquitin chains that interact with NEMO to facilitate activation of the canonical IKK complex by TAK1. ADP-heptose additionally stimulates the activation of TBK1, which can be mediated by either TRAF6 or TRAF2 via an unknown pathway that does not require TAK1. TBK1 is likely to function as a negative feedback regulator of the pathway to prevent the overproduction of inflammatory mediators. The phosphorylation of TIFA at Thr177 also appears to be a feedback control device to suppress the TRAF6-dependent arm of the pathway. TBK1 may function at least in part, to restrict the activation of the canonical IKK complex. By analogy with IL-1 and TLR signalling, the K63-Ub and M1-Ub chains are depicted as being linked to one another, although this has not yet been established for the ADP-H signalling pathway. The degradation of TIFA (not shown) may also contribute to the feedback control of ADP-heptose signalling.

Materials and methods

Antibodies

The following antibodies were obtained from Cell Signalling Technology (CST): phospho-specific antibodies recognising IKKα phosphorylated at Ser176 and Ser180 and IKKβ phosphorylated at Ser177 and Ser181 (#2697), p38α MAPK and p38γ MAPK phosphorylated at Thr180 and Tyr182 within their Thr-Gly-Tyr motifs (#9211), JNK1 and JNK2 phosphorylated at Thr183 and Thr185 within their Thr-Pro-Tyr motifs (#9251), TAK1 phosphorylated at Thr187 (#4536), TBK1 phosphorylated at Ser172 (#5483) and IKKε phosphorylated at Ser172 (#8766) (these are the phosphorylation sites within the activation loops that trigger the activation of these protein kinases); the IKKβ substrate NF-κB1 (also called p105) phosphorylated at Ser133 (#4806). Also from CST were antibodies recognising anti-rabbit IgG (#7074) and anti-mouse IgG (#7076), FLAG (#2368), GAPDH (#2118), human c-IAP1 (#7065), human c-IAP2 (#3130), IκBα (#4812), IKKβ (#8943), IRAK1 (#4504), NIK (#4994), Pellino 1 (#31474), human TIFA (#61358), TRAF2 (#4712) and human TRAF6 (#8028). An Antibody recognising anti-human IgG (#2040-05) was from Southern Biotech and anti-rat IgG (#405405) from Biolegend. Anti-sheep IgG (#ab97130) and murine TRAF6 (#ab40675) were from Abcam and murine c-IAP1 (#803-335-C100) was from Enzo Life Sciences. Antibodies recognising Met1-linked ubiquitin and Lys63-linked ubiquitin were generous gifts from Vishva Dixit (Genentech). Antibodies against ALPK1[1–358] (S593D, bleed 5) and ALPK1[395–823] (S594D, bleed 3) were raised in sheep by the MRC Reagents and Services section of the MRC Protein Phosphorylation and Ubiquitylation Unit, the University of Dundee and are available on request (mrcppureagents.dundee.ac.uk). The molecular mass markers needed to gauge the size of each band identified by immunoblotting with these antibodies are shown in Supplementary Figure S7.

DNA constructs

The following DNA vectors for expression in mammalian cells were made by the DNA cloning team of MRC Reagents and Services, MRC Protein Phosphorylation and Ubiquitylation Unit, University of Dundee and are available on request (mrcppureagents.dundee.ac.uk). For the generation of stable cell lines using pBabe and pRetroXTight vectors: TRAF6 (DU47223), FLAG-TRAF6 (DU32495), TRAF6[L74H] (DU47224), TRAF6[120–522] (DU51445), TAK1 (DU51270) and TAK1 [D175A] (DU51293). For transient transfection: FLAG-ALPK1 (DU65668, CMV promoter), FLAG-ALPK1 (DU65976, UbC promoter), FLAG-ALPK1[K1067M] (DU65680, CMV promoter), FLAG-ALPK1[K1067M] (DU71020, UbC promoter), FLAG-TIFA (DU71017, UbC promoter), FLAG-TIFA[T9A] (DU71055, UbC promoter), FLAG-TIFA[T9D] (DU71053), FLAG-TIFA[T9E] (DU71054, UbC promoter), FLAG-TIFA[T9S] (DU71067, UbC promoter), FLAG-TIFA[T177A] (DU71049, UbC promoter), FLAG-TIFA[T177D] (DU71051, UbC promoter) and FLAG-TIFA[E178A] (DU71057, UbC promoter). The plasmids with a CMV promoter were used for the purification of proteins, whereas those with the weaker UbC promoter [53] were used for the study of intracellular signalling.

The procedure and guide sequences for the removal of TAK1 or TRAF6 are described elsewhere [23,54]. The guides for the removal of TRAF2 were GACCCTCCTGGGGACCAAGC (Sense, DU52594) and GCCGGGCTGTAGCAACTCCA (Antisense, DU52604).

Proteins

Glutathione-S-transferase (GST)-tagged proteins contained a PreScission protease cleavage site between the GST and the protein of interest: GST-TIFA (DU2421), GST-TIFA[T9A] (DU65850) and GST-TIFA[T9S] (DU65858). These proteins were produced by the MRC Protein Phosphorylation and Ubiquitylation Unit's reagents section and are available on request (mrcppureagents.dundee.ac.uk). Halo-NEMO (DU35939) was expressed and coupled to Halo-link resin as described [38].

Cell culture, cell maintenance and cell lysis

HEK293 cells stably expressing relatively low levels of the IL-1 receptor, termed IL-1R* HEK293 cells, have been described [23]. ALPK1 knockout and TIFA knockout HEK293 cells and their parental cell line were purchased from Invivogen and termed HEK293 cells. HEK293 cells were cultured at 37°C in a humidified atmosphere containing 5% CO_2. The growth media contained Dulbecco's modified Eagle's medium (DMEM), containing 25 mM HEPES pH 7.3, 10% (v/v) foetal bovine serum (FBS), 2 mM L-glutamine, 100 U/ml penicillin and 0.1 mg/ml streptomycin. BMDM were obtained by differentiating bone marrow extracted from the femur and tibia of mice and cultured as described [55]. Since few TRAF6 KO mice are born alive and those

that do die within days, macrophages from TRAF6 KO mice were produced from foetal liver cells and cultured as described [23]. The preparation and culture of MEFs from HOIP[C879S] and NEMO[D311N] mice were described previously and was cultured as described [22]. Cells were washed twice with ice-cold PBS, scraped from the plate in lysis buffer (50 mM Tris–HCl pH 7.5, 1 mM EDTA, 1 mM EGTA, 1% (v/v) Triton X-100, 1 mM sodium orthovanadate, 50 mM sodium fluoride, 5 mM sodium pyrophosphate, 270 mM sucrose, 10 mM sodium 2-glycerophosphate, 0.2 mM phenylmethylsulfonyl fluoride and 1 mM benzamidine, supplemented with complete protease inhibitor cocktail). When studying ubiquitin chain formation, 100 mM iodoacetamide was included to inhibit deubiquitylases (DUBs) [56]. Cell lysates were clarified by centrifugation for 20 min at 20 000×g at 4°C and the supernatants (cell extracts) transferred to 1.5 ml microcentrifuge tubes, snap frozen and stored at −80°C. The protein concentrations of cell extracts were determined by the Bradford procedure.

Transient transfection of HEK293 cells
HEK293 cells were transfected in 10 cm dishes at 70% confluency using lipofectamine 2000 according to the manufacturer's instructions.

Generation of retroviruses using HEK293FT cells and infection of target cells
HEK293FT cells were plated on 10 cm dishes pre-coated with poly-L-lysine. Transfection was performed at 90% confluency using Lipofectamine LTX according to the manufacturer's instructions. Retroviral particles were prepared using pBabe and pRetroXTight vectors as described elsewhere [23,54]. HEK293 cells in 6-well plates were infected at 50% confluency using 500 μl of viral suspension and 8 μg/ml polybrene. The media was replaced 24 h later and after a further 24 h, the retrovirally transduced cells were selected for stable integration of the protein of interest using media containing 2 μg/ml puromycin and/or 1 mg/ml G418.

Mice
TRAF6[L74H] knock-in mice were produced as described [23] and heterozygous TRAF6 KO mice were provided by Tak Mak. Mice were maintained on a C57BL/6 background and provided with free access to food and water. Animals were kept in ventilated cages under specific pathogen-free conditions in accordance with U.K. and European Union regulations. Experiments were carried out subject to approval by the University of Dundee ethical review board under a U.K. Home Office project licence.

Agonists and inhibitors
ADP-D,D-heptose and ADP-L,D-heptose was synthesised as described [57] and were free of endotoxin contamination as judged by the QCLTM Kinetic Chromogenic LAL Assay (Lonza). The ADP-heptoses, Resiquimod (R848) (Invivogen) and human IL-1β (Invivogen) were dissolved in PBS and added to the cell culture medium to achieve final concentrations of 10 μM (ADP-heptose), 250 ng/ml (R848) and 5 ng/ml (IL-1β). NG-25 and BV-6 (from SelleckChem) and (5Z)-7-Oxozeaenol (from Tocris) were dissolved in DMSO at 10 mM and added to achieve the final concentrations indicated in figure legends. An equivalent volume of DMSO was added to the culture medium in control incubations.

SDS–PAGE, transfer to PVDF membranes and immunoblotting
Cell extracts (20 μg of protein) or immunoprecipitates were resolved by SDS–PAGE and transferred to PVDF membranes (Merck-Millipore, #10344661) using a Trans-Blot transfer cell (Bio-Rad). The membranes were blocked by incubation for 1 h in 50 mM Tris–HCl pH 7.5, 150 mM NaCl and 0.1% (v/v) Tween-20 (TBS-T) containing 5% (w/v) non-fat milk powder (Marvel). Primary antibody in TBS-T containing 5% (w/v) bovine serum albumin was then incubated with the PVDF membrane on a shaker for 16 h at 4°C. The immunoblots were washed five times (10 min per wash) with TBS-T followed by incubation for 1 h with the appropriate horseradish peroxidase-conjugated secondary antibody in TBS-T containing 5% (w/v) non-fat milk powder and washed a further five times with TBS-T. Most blots were developed by incubation at ambient temperature with Amersham ECL Select Western Blotting Detection Reagent (GE Healthcare) or Super-Signal West Pico Chemiluminescent Substrate (Merck-Millipore). The most sensitive reagent, Clarity Max Western ECL Substrate (Bio-Rad), was used to blot for ubiquitylated proteins. Most immunoblots were imaged using a ChemiDoc MP scanner (#17001402, Bio-Rad). Ubiquitin blots were exposed to Amersham Hyperfilm X-ray film in an X-ray cassette and developed using a Konica automatic developer. Antibodies were stripped from membranes by incubation for 15 min at ambient temperature with Restore Western Blot Stripping Buffer

(Thermo Fisher). The stripped membranes were washed twice with TBS-T and immunoblotting repeated by incubation with a different primary antibody.

Immunoprecipitation of endogenous ALPK1

Cell extracts (1 mg protein) were treated for 15 min at ambient temperature with benzonase (Merck-Millipore) and pre-cleared by incubation for 30 min at 4°C with 20 μl of protein A/G-Sepharose beads. ALPK1[1–358] antibody (10 μg) was added to the supernatant and incubated for 1 h at 4°C on a rotating wheel followed by the addition of 20 μl protein A/G-Sepharose for 30 min. After brief centrifugation, the supernatant was discarded and the beads washed twice with 50 mM Tris–HCl pH 7.5, 1% (v/v) Triton X-100 and 500 mM NaCl and then twice with 50 mM Tris–HCl pH 7.5, 1% (v/v) Triton X-100. The immunoprecipitated ALPK1 was released by incubation for 5 min at 95°C with LDS sample buffer (Thermo Fisher, #NP0007) containing 2.5% (v/v) β-mercaptoethanol. The suspension was transferred to Spin-X columns (Corning, #8162), centrifuged for 1 min at 20 000×g and the flowthrough was analysed by SDS–PAGE and immunoblotted with an antibody recognising ALPK1[395–823].

Halo-NEMO pulldowns

Packed Halo-NEMO resin (20 μl) was added to cell extracts (2 mg protein) and incubated for 4 h at 4°C on a rotating wheel to capture Met1/Lys63-linked ubiquitin chains and the proteins to which they were attached covalently and non-covalently. The resin was washed twice with 50 mM Tris–HCl pH 7.5, 1% (v/v) Triton X-100 and 500 mM NaCl and twice with 50 mM Tris–HCl pH 7.5, 1% (v/v) Triton X-100 to remove proteins attached non-specifically to the resin. Proteins captured on the resin were released by incubation for 10 min at 37°C in LDS sample buffer containing 2.5% (v/v) β-mercaptoethanol. The suspension was transferred to Spin-X columns (Corning, #8162), centrifuged for 1 min at 20 000×g and the flowthrough was analysed by SDS–PAGE.

Immunoprecipitation of FLAG-tagged proteins

To identify proteins interacting with TRAF6 by MS, HEK293 cells stably expressing FLAG-TRAF6 were either left untreated, stimulated for 15 min with IL-1β or ADP-heptose. Cells were lysed in ice-cold lysis buffer containing 100 mM iodoacetamide, centrifuged (30 min at 20 000×g at 4°C) and the cell extracts passed through 0.45 μm filters. The supernatants from unstimulated, IL-1β- and ADP-heptose-stimulated cells (30 mg protein per condition) were diluted to 2 mg/ml protein with lysis buffer and pre-cleared by incubation for 12 h at 4°C on a rotating wheel with mouse IgG-agarose. The supernatants were collected and incubated for 4 h at 4°C on a rotating wheel with 40 μl of packed anti-FLAG M2 affinity gel (Sigma, #A2220), which had been washed three times with lysis buffer prior to use. After centrifugation, the supernatant was discarded and the pelleted gel washed three times with 50 mM Tris–HCl pH 7.5, 1% (v/v) Triton X-100 containing 300 mM NaCl and twice with 50 mM Tris–HCl (pH 7.5), 1% (v/v) Triton X-100. The proteins captured on the anti-FLAG resin were eluted by incubation with 46 μl of TBS containing 150 ng/μl of 3X FLAG peptide (Sigma, #F4799). For MS analysis the above procedure was repeated 5 times for each of the three conditions, giving a total of 15 samples.

FLAG-ALPK1 or FLAG-TIFA were transiently re-expressed in ALPK1 KO or TIFA KO HEK293 cells, respectively, for 48 h unless stated otherwise and the proteins were immunoprecipitated with anti-FLAG and washed as described above, except that 0.2–1 mg of cell extract protein and 20 μl of resin and elution from the anti-FLAG gel was achieved using LDS sample buffer as described earlier. To identify sites on TIFA phosphorylated by FLAG-ALPK1, the FLAG-ALPK1 was immunoprecipitated as described above but washed with 500 mM instead of 300 mM NaCl.

Phosphorylation of TIFA by ALPK1 *in vitro*

GST-TIFA was phosphorylated using FLAG-ALPK1 attached to the anti-FLAG resin and carried out for 20 min in 25 μl of 50 mM Tris–HCl pH 7.5, 2 mM DTT, 0.1 mM EGTA, 8 μM GST-TIFA, 100 nM ADP-heptose, 10 mM magnesium acetate and 0.1 mM [γ-^{32}P]ATP (specific radioactivity 1000 cpm/pmol). Reactions were terminated using LDS sample buffer containing 2.5% (v/v) β-mercaptoethanol and heated for 5 min at 75°C. The resin was pelleted by brief centrifugation at 13 000×g and half of the supernatant subjected to SDS–PAGE. After staining for 1 h with Instant Blue and destaining in water for 48 h, incorporation of ^{32}P-radioactivity into TIFA and ALPK1 was analysed by autoradiography and Cerenkov counting.

Identification of phosphorylation sites in TIFA

To identify the sites on TIFA phosphorylated by FLAG-ALPK1, GST-TIFA and GST-TIFA[T9A] were cleaved with PreScission protease, and passed through glutathione-Sepharose to remove GST, prior to phosphorylation. The purified TIFA preparations began with the linker sequence GLPGS followed by amino acid residues 2–184 of TIFA. Following phosphorylation for 20 min, the ^{32}P-labelled band corresponding to phosphorylated TIFA was excised, cut into many sections and washed with 50 mM Tris–HCl pH 8.0 containing 50% (v/v) aceto-nitrile until the gel pieces were colourless as described previously [58]. The gel pieces were then incubated for 30 min at ambient temperature with 100 mM triethyl ammonium bicarbonate (TEAB) containing 10 mM dithiothreitol and alkylated in the dark for 30 min at ambient temperature in 50 mM iodoacetamide. The gel pieces were resuspended in 0.1 ml of 100 mM Tris–HCl pH 8.0 containing 10 mM calcium chloride and chymotrypsin (Promega, #V1061) for 16 h at 25°C. The resulting peptides were collected and separated on a reverse-phase Vydac C_{18} column (Separations Group, CA, U.S.A.) with on-line radioactivity detection. The column was equilibrated in 0.1% (v/v) trifluoroacetic acid and developed with a linear acetonitrile gradient at a flow rate of 0.2 ml/min. Fractions (0.1 ml) were collected and analysed for ^{32}P-radioactivity by Cerenkov count-ing. The identified phosphopeptide fractions were analysed by liquid chromatography (LC)-MS/MS using a Thermo U3000 RSLC nano LC system or an EvoSep LC coupled to an Exploris 240 mass spectrometer (Thermo Fisher) to determine the primary sequence of the phospho-peptides. Data files were searched using Mascot (www.matrixscience.com) with a 10 ppm mass accuracy for precursor ions, a 0.06 Da tolerance for frag-ment ions, and allowing for Phospho (ST), Phospho (Y) and oxidation of methionine (M) as variable modifica-tions. Individual MS/MS spectra were inspected using Xcalibur 2.2 and Proteome Discoverer with phosphoRS 3.1 (Thermo Fisher) was used to assist the assignment of phosphorylation sites. The sites of phosphorylation of ^{32}P-labeled peptides were also determined by solid phase Edman degradation on a Shimadzu PPSQ33A Sequencer (Kyoto, Japan) with the peptides coupled to an 80 Sequelon-AA membrane (Applied Biosystems), as described [59].

TMT labelling and mass spectrometry

The Flag-TRAF6 preparations eluted from FLAG resin with 3X FLAG peptide were digested with a combin-ation of trypsin and Lys-C protease (Promega, #V5071) using S-trap mini columns (Protifi) according to the manufacturer's instructions, except that 20 mM iodoacetamide was used for alkylation and washing steps with 100 mM TEAB in 90% (v/v) methanol repeated 10 times to remove traces of Tris buffer that would otherwise interfere with TMT labelling. The resultant peptides were resuspended for 15-plex TMT labelling according to the manufacturer's protocol (Thermo Fisher) and the 15 samples (see the preceding section) were combined in equimolar amounts and dried. Peptides were resuspended in 100 µl of 5 mM ammonium acetate at pH 10 and injected on to a XBridge Peptide BEH C_{18} column (Waters #186003561). Peptides were eluted from the column using basic reverse phase fractionation (using 10 mM ammonium acetate in water as Buffer A and 10 mM ammonium acetate in 80:20 (v/v) acetonitrile:water as Buffer B) on a 55 min multistep gradient at 100 µl/min. Eluted peptides were collected into 96 fractions, pooled into 24 fractions using non-consecutive concatenation and dried. The peptides were redissolved in 5% (v/v) formic acid and injected on an UltiMate 3000 RSLCnano System coupled to a Orbitrap Fusion Lumos Tribrid Mass Spectrometer (Thermo Fisher). Peptides were loaded on to an Acclaim Pepmap trap column (Thermo Fisher #164564-CMD) prior to analysis on a PepMap RSLC C18 analytical column (Thermo Fisher #ES903) and eluted using a 120 min linear gradient from 3% to 35% Buffer B (Buffer A: 0.1% formic acid, Buffer B: 0.08% formic acid in 80:20 (v/v) acetonitrile: water. The eluted peptides were then analysed by the mass spectrometer operating in synchronous precursor selection (SPS) mode on a TOP 3s method.

Analysis of TMT MS data

A peptide search was conducted by interrogating the Uniprot Swissprot Human database (released on 05/10/2021) using MaxQuant 1.6.17.0 in MS3 reporter ion mode. using default parameters with the addition of dea-midation (NQ) and phospho (STY) as variable modifications. Protein groups present in the reversed database, or a database of proteins that are frequent contaminants, or proteins in which only one unique peptide or razor peptide were detected, or proteins present in less than 4 of the 5 replicates were excluded. Missing values were then imputed using a Gaussian distribution centred on the median with a downshift of 1.8 and width of 0.3 (based on the standard deviation) and protein intensities were median normalised. Protein regulation was

assessed using a two sample Welch test and *P*-values were adjusted using Benjamini–Hochberg (BH) multiple hypothesis correction. Proteins in TRAF6 immunoprecipitates were considered to be enriched significantly after cell stimulation with ADP-heptose if the BH corrected P-value was smaller than 0.05 and the fold-change was greater than 1.75. The MS proteomics data have been deposited to the ProteomeXchange Consortium via the PRIDE [60] partner repository with the dataset identifier PXD034964.

Data Availability
The mass spectrometry proteomics data have been deposited to the ProteomeXchange Consortium via the PRIDE partner repository with the dataset identifier PXD034964. All other data has been provided in the main article or as Supplementary material.

Competing Interests
The authors declare that there are no competing interests associated with the manuscript.

CRediT Author Contribution
Philip Cohen: Conceptualization, Supervision, Funding acquisition, Writing — original draft, Project administration, Writing — review and editing. **Tom Snelling**: Conceptualization, Data curation, Formal analysis, Investigation, Visualization, Writing — original draft, Writing — review and editing. **Natalia Shpiro**: Resources. **Robert Gourlay**: Investigation. **Frederic Lamoliatte**: Formal analysis, Investigation.

Abbreviations
ALPK1, alpha-protein kinase 1; BMDM, bone marrow-derived macrophages; CST, Cell Signalling Technology; GST, glutathione-S-transferase; HEK, human embryonic kidney; IKK, IκB kinase; IL-1, Interleukin-1; KO, knockout; LC, liquid chromatography; LUBAC, linear ubiquitin assembly complex; M1-Ub, Met1-linked ubiquitin; MAPKs, mitogen-activated protein kinases; MEFs, mouse embryonic fibroblasts; MS, mass spectrometry; MS, mass spectrometry; PRRs, pattern recognition receptors; T2BP, TRAF2-binding protein; TBK1, TANK-binding kinase-1; TEAB, triethyl ammonium bicarbonate; TIFA, TRAF-interacting protein with FHA domain; TLRs, Toll-like receptors; TMT, tandem mass tag; TRAF, TNF receptor-activating factor; WT, wild-type.

References
1 Medzhitov, R. (2007) Recognition of microorganisms and activation of the immune response. *Nature* **449**, 819–826 https://doi.org/10.1038/nature06246
2 Stein, S.C., Faber, E., Bats, S.H., Murillo, T., Speidel, Y., Coombs, N. et al. (2017) Helicobacter pylori modulates host cell responses by CagT4SS-dependent translocation of an intermediate metabolite of LPS inner core heptose biosynthesis. *PLoS Pathog.* **13**, e1006514 https://doi.org/10.1371/journal.ppat.1006514
3 Schäffer, C. and Messner, P. (2004) Surface-layer glycoproteins: an example for the diversity of bacterial glycosylation with promising impacts on nanobiotechnology. *Glycobiology* **14**, 31R–42R https://doi.org/10.1093/glycob/cwh064
4 Tang, W., Guo, Z., Cao, Z., Wang, M., Li, P., Meng, X., et al. (2018) D-Sedoheptulose-7-phosphate is a common precursor for the heptoses of septacidin and hygromycin B. *Proc. Natl Acad. Sci. U.S.A.* **115**, 2818–2823 https://doi.org/10.1073/pnas.1711665115
5 Zhou, P., She, Y., Dong, N., Li, P., He, H., Borio, A., et al. (2018) Alpha-kinase 1 is a cytosolic innate immune receptor for bacterial ADP-heptose. *Nature* **561**, 122–126 https://doi.org/10.1038/s41586-018-0433-3
6 Kanamori, M., Suzuki, H., Saito, R., Muramatsu, M. and Hayashizaki, Y. (2002) T2BP, a novel TRAF2 binding protein, can activate NF-κB and AP-1 without TNF stimulation. *Biochem. Biophys. Res. Commun.* **290**, 1108–1113 https://doi.org/10.1006/bbrc.2001.6315
7 Tada, K., Okazaki, T., Sakon, S., Kobarai, T., Kurosawa, K., Yamaoka, S., et al. (2001) Critical roles of TRAF2 and TRAF5 in tumor necrosis factor-induced NF-kappa B activation and protection from cell death. *J. Biol. Chem.* **276**, 36530–36534 https://doi.org/10.1074/jbc.M104837200

8   Takatsuna, H., Kato, H., Gohda, J., Akiyama, T., Moriya, A., Okamoto, Y., et al. (2003) Identification of TIFA as an adapter protein that links tumor necrosis factor receptor-associated factor 6 (TRAF6) to Interleukin-1 (IL-1) receptor-associated kinase-1 (IRAK-1) in IL-1 receptor signaling. *J. Biol. Chem.* **278**, 12144–12150 https://doi.org/10.1074/jbc.M300720200

9   Ea, C.K., Sun, L., Inoue, J.I. and Chen, Z.J. (2004) TIFA activates IκB kinase (IKK) by promoting oligomerization and ubiquitination of TRAF6. *Proc. Natl Acad. Sci. U.S.A.* **101**, 15318–15323 https://doi.org/10.1073/pnas.0404132101

10   Mahajan, A., Yuan, C., Lee, H., Chen, E.S.W., Wu, P.Y. and Tsai, M.D. (2008) Structure and function of the phosphothreonine-specific FHA domain. *Sci. Signal.* **1**, re12 https://doi.org/10.1126/scisignal.151re12

11   Fang, C.Y., Chen, H.Y., Wang, M., Chen, P.L., Chang, C.F., Chen, L.S., et al. (2010) Global analysis of modifications of the human BK virus structural proteins by LC-MS/MS. *Virology* **402**, 164–176 https://doi.org/10.1016/j.virol.2010.03.029

12   Huang, C.-C.F., Weng, J.-H., Wei, T.-Y.W., Wu, P.-Y.G., Hsu, P.-H., Chen, Y.-H., et al. (2012) Intermolecular binding between TIFA-FHA and TIFA-pT mediates tumor necrosis factor alpha stimulation and NF-κB activation. *Mol. Cell. Biol.* **32**, 3800–3800 https://doi.org/10.1128/MCB.00985-12

13   Gaudet, R.G., Sintsova, A., Buckwalter, C.M., Leung, N., Cochrane, A., Li, J. et al. (2015) Cytosolic detection of the bacterial metabolite HBP activates TIFA-dependent innate immunity. *Science* **348**, 1251–1255 https://doi.org/10.1126/science.aaa4921

14   Gall, A., Gaudet, R.G., Gray-Owen, S.D. and Salama, N.R. (2017) TIFA signaling in gastric epithelial cells initiates the cag type 4 secretion system-dependent innate immune response to helicobacter pylori infection. *MBio* **8**, e01168-17 https://doi.org/10.1128/mBio.01168-17

15   Milivojevic, M., Dangeard, A.S., Kasper, C.A., Tschon, T., Emmenlauer, M., Pique, C. et al. (2017) ALPK1 controls TIFA/TRAF6-dependent innate immunity against heptose-1,7-bisphosphate of gram-negative bacteria. *PLoS Pathog.* **13**, e1006224 https://doi.org/10.1371/journal.ppat.1006224

16   Zimmermann, S., Pfannkuch, L., Al-Zeer, M.A., Bartfeld, S., Koch, M., Liu, J., et al. (2017) ALPK1- and TIFA-dependent innate immune response triggered by the *Helicobacter pylori* type IV secretion system. *Cell Rep.* **20**, 2384–2395 https://doi.org/10.1016/j.celrep.2017.08.039

17   Boulard, O., Kirchberger, S., Royston, D.J., Maloy, K.J. and Powrie, F.M. (2012) Identification of a genetic locus controlling bacteria-driven colitis and associated cancer through effects on innate inflammation. *J. Exp. Med.* **209**, 1309–1324 https://doi.org/10.1084/jem.20120239

18   Ryzhakov, G., West, N.R., Franchini, F., Clare, S., Ilott, N.E., Sansom, S.N., et al. (2018) Alpha kinase 1 controls intestinal inflammation by suppressing the IL-12/Th1 axis. *Nat. Commun.* **9**, 1–13 https://doi.org/10.1038/s41467-018-06085-5

19   Waterfield, M., Jin, W., Reiley, W., Zhang, M. and Sun, S.-C. (2004) Iκb kinase is an essential component of the Tpl2 signaling pathway. *Mol. Cell. Biol.* **24**, 6040–6048 https://doi.org/10.1128/MCB.24.13.6040-6048.2004

20   Beinke, S., Robinson, M.J., Hugunin, M. and Ley, S.C. (2004) Lipopolysaccharide activation of the TPL-2/MEK/extracellular signal-regulated kinase mitogen-activated protein kinase cascade is regulated by IkappaB kinase-induced proteolysis of NF-kappaB1 p105. *Mol. Cell. Biol.* **24**, 9658–9667 https://doi.org/10.1128/MCB.24.21.9658-9667.2004

21   Yamamoto, Y., Yin, M.-J. and Gaynor, R.B. (2000) Ikappab kinase alpha (IKKalpha) regulation of IKKbeta kinase activity. *Mol. Cell. Biol.* **20**, 3655–3666 https://doi.org/10.1128/MCB.20.10.3655-3666.2000

22   Zhang, J., Clark, K., Lawrence, T., Peggie, M.W., Cohen, P., Zhang, J. et al. (2014) An unexpected twist to the activation of IKKβ: TAK1 primes IKKβ for activation by autophosphorylation. *Biochem. J.* **461**, 531–537 https://doi.org/10.1042/BJ20140444

23   Strickson, S., Emmerich, C.H., Goh, E.T.H., Zhang, J., Kelsall, I.R., MacArtney, T., et al. (2017) Roles of the TRAF6 and Pellino E3 ligases in MyD88 and RANKL signaling. *Proc. Natl Acad. Sci. U.S.A.* **114**, E3481–E3489 https://doi.org/10.1073/pnas.1702367114

24   Ninomiya-Tsuji, J., Kajino, T., Ono, K., Ohtomo, T., Matsumoto, M., Shiina, M. et al. (2003) A resorcylic acid lactone, 5Z-7-oxozeaenol, prevents inflammation by inhibiting the catalytic activity of TAK1 MAPK kinase kinase. *J. Biol. Chem.* **278**, 18485–18490 https://doi.org/10.1074/jbc.M207453200

25   Tan, L., Nomanbhoy, T., Gurbani, D., Patricelli, M., Hunter, J., Geng, J., et al. (2015) Discovery of type II inhibitors of TGFβ-activated kinase 1 (TAK1) and mitogen-activated protein kinase kinase kinase 2 (MAP4K2). *J. Med. Chem.* **58**, 183–196 https://doi.org/10.1021/jm500480k

26   Kanayama, A., Seth, R.B., Sun, L., Ea, C.K., Hong, M., Shaito, A. et al. (2004) TAB2 and TAB3 activate the NF-κB pathway through binding to polyubiquitin chains. *Mol. Cell* **15**, 535–548 https://doi.org/10.1016/j.molcel.2004.08.008

27   Kulathu, Y., Akutsu, M., Bremm, A., Hofmann, K. and Komander, D. (2009) Two-sided ubiquitin binding explains specificity of the TAB2 NZF domain. *Nat. Struct. Mol. Biol.* **16**, 1328–1330 https://doi.org/10.1038/nsmb.1731

28   Kirisako, T., Kamei, K., Murata, S., Kato, M., Fukumoto, H., Kanie, M. et al. (2006) A ubiquitin ligase complex assembles linear polyubiquitin chains. *EMBO J.* **25**, 4877–4887 https://doi.org/10.1038/sj.emboj.7601360

29   Tokunaga, F., Sakata, S.I., Saeki, Y., Satomi, Y., Kirisako, T., Kamei, K., et al. (2009) Involvement of linear polyubiquitylation of NEMO in NF-κB activation. *Nat. Cell Biol.* **11**, 123–132 https://doi.org/10.1038/ncb1821

30   Lo, Y.C., Lin, S.C., Rospigliosi, C.C., Conze, D.B., Wu, C.J., Ashwell, J.D. et al. (2009) Structural basis for recognition of diubiquitins by NEMO. *Mol. Cell* **33**, 602–615 https://doi.org/10.1016/j.molcel.2009.01.012

31   Rahighi, S., Ikeda, F., Kawasaki, M., Akutsu, M., Suzuki, N., Kato, R., et al. (2009) Specific recognition of linear ubiquitin chains by NEMO is important for NF-kappaB activation. *Cell* **136**, 1098–1109 https://doi.org/10.1016/j.cell.2009.03.007

32   Smith, H., Peggie, M., Campbell, D.G., Vandermoere, F., Carrick, E. and Cohen, P. (2009) Identification of the phosphorylation sites on the E3 ubiquitin ligase Pellino that are critical for activation by IRAK1 and IRAK4. *Proc. Natl Acad. Sci. U.S.A.* **106**, 4584–4590 https://doi.org/10.1073/pnas.0900774106

33   Goh, E.T.H., Arthur, J.S.C., Cheung, P.C.F., Akira, S., Toth, R. and Cohen, P. (2012) Identification of the protein kinases that activate the E3 ubiquitin ligase Pellino 1 in the innate immune system. *Biochem. J.* **441**, 339–346 https://doi.org/10.1042/BJ20111415

34   Ordureau, A., Smith, H., Windheim, M., Peggie, M., Carrick, E., Morrice, N. et al. (2008) The IRAK-catalysed activation of the E3 ligase function of Pellino isoforms induces the Lys63-linked polyubiquitination of IRAK1. *Biochem. J.* **409**, 43–52 https://doi.org/10.1042/BJ20071365

35   Cohen, P. and Strickson, S. (2017) The role of hybrid ubiquitin chains in the MyD88 and other innate immune signalling pathways. *Cell Death Differ.* **24**, 1153–1159 https://doi.org/10.1038/cdd.2017.17

36   Schaeffer, V., Akutsu, M., Olma, M.H., Gomes, L.C., Kawasaki, M. and Dikic, I. (2014) Binding of OTULIN to the PUB domain of HOIP controls NF-κB signaling. *Mol. Cell* **54**, 349–361 https://doi.org/10.1016/j.molcel.2014.03.016

37   Duckett, C.S. (2005) IAP proteins: sticking it to Smac. *Biochem. J.* **385**, 1–2 https://doi.org/10.1042/BJ20041800

38   Emmerich, C.H., Ordureau, A., Strickson, S., Arthur, J.S.C., Pedrioli, P.G.A.A., Komander, D. et al. (2013) Activation of the canonical IKK complex by K63/M1-linked hybrid ubiquitin chains. *Proc. Natl Acad. Sci. U.S.A.* **110**, 15247–15252 https://doi.org/10.1073/pnas.1314715110

39   Yin, Q., Lin, S.-C., Lamothe, B., Lu, M., Lo, Y.-C., Hura, G., et al. (2009) E2 interaction and dimerization in the crystal structure of TRAF6. *Nat. Struct. Mol. Biol.* **16**, 658–666 https://doi.org/10.1038/nsmb.1605

40   Li, W., Li, B., Giacalone, N.J., Torossian, A., Sun, Y., Niu, K. et al. (2011) BV6, an IAP antagonist, activates apoptosis and enhances radiosensitization of non-small cell lung carcinoma in vitro. *J. Thorac. Oncol.* **6**, 1801 https://doi.org/10.1097/JTO.0b013e318226b4a6

41   Wang, S. (2010) Design of small-molecule Smac mimetics as IAP antagonists. *Curr. Top. Microbiol. Immunol.* **348**, 89–113 https://doi.org/10.1007/82_20210_111

42   Sun, S.C. (2017) The non-canonical NF-κB pathway in immunity and inflammation. *Nat. Rev. Immunol.* **17**, 545–558 https://doi.org/10.1038/nri.2017.52

43   Maubach, G., Lim, M.C.C., Sokolova, O., Backert, S., Meyer, T.F. and Naumann, M. (2021) TIFA has dual functions in *Helicobacter pylori*-induced classical and alternative NF-κB pathways. *EMBO Rep.* **22**, e52878 https://doi.org/10.15252/embr.202152878

44   Kishore, N., Khai Huynh, Q., Mathialagan, S., Hall, T., Rouw, S., Creely, D., et al. (2002) IKK-i and TBK-1 are enzymatically distinct from the homologous enzyme IKK-2: comparative analysis of recombinant human IKK-i, TBK-1, and IKK-2. *J. Biol. Chem.* **277**, 13840–13847 https://doi.org/10.1074/jbc.M110474200

45   Ye, H., Arron, J.R., Lamothe, B., Cirilli, M., Kobayashi, T., Shevde, N.K., et al. (2002) Distinct molecular mechanism for initiating TRAF6 signalling. *Nature* **418**, 443–447 https://doi.org/10.1038/nature00888

46   Middleton, A.J., Budhidarmo, R., Das, A., Zhu, J., Foglizzo, M., Mace, P.D. et al. (2017) The activity of TRAF RING homo- and heterodimers is regulated by zinc finger 1. *Nat. Commun.* **8**, 1–10 https://doi.org/10.1038/s41467-017-01665-3

47   Wang, C., Deng, L., Hong, M., Akkaraju, G.R., Inoue, J.I. and Chen, Z.J. (2001) TAK1 is a ubiquitin-dependent kinase of MKK and IKK. *Nature* **412**, 346–351 https://doi.org/10.1038/35085597

48   Walsh, M.C., Kim, G.K., Maurizio, P.L., Molnar, E.E. and Choi, Y. (2008) TRAF6 autoubiquitination-independent activation of the NFκB and MAPK pathways in response to IL-1 and RANKL. *PLoS One* **3**, e4064 https://doi.org/10.1371/journal.pone.0004064

49   Clark, K., Peggie, M., Plater, L., Sorcek, R.J., Young, E.R.R., Madwed, J.B. et al. (2011) Novel cross-talk within the IKK family controls innate immunity. *Biochem. J.* **434**, 93–104 https://doi.org/10.1042/BJ20101701

50   Palkowitsch, L., Leidner, J., Ghosh, S. and Marienfeld, R.B. (2008) Phosphorylation of serine 68 in the IkappaB kinase (IKK)-binding domain of NEMO interferes with the structure of the IKK complex and tumor necrosis factor-alpha-induced NF-kappaB activity. *J. Biol. Chem.* **283**, 76–86 https://doi.org/10.1074/jbc.M708856200

51   Delhase, M., Makio, H., Chen, Y. and Karin, M. (1999) Positive and negative regulation of IκB kinase activity through IKKβ subunit phosphorylation. *Science* **284**, 309–313 https://doi.org/10.1126/science.284.5412.309

52   Ye, H., Park, Y.C., Kreishman, M., Kieff, E. and Wu, H. (1999) The structural basis for the recognition of diverse receptor sequences by TRAF2. *Mol. Cell* **4**, 321–330 https://doi.org/10.1016/S1097-2765(00)80334-2

53   Qin, J.Y., Zhang, L., Clift, K.L., Hulur, I., Xiang, A.P., Ren, B.Z. et al. (2010) Systematic comparison of constitutive promoters and the doxycycline-inducible promoter. *PLoS One* **5**, e10611 https://doi.org/10.1371/journal.pone.0010611

54   Zhang, J., Macartney, T., Peggie, M. and Cohen, P. (2017) Interleukin-1 and TRAF6-dependent activation of TAK1 in the absence of TAB2 and TAB3. *Biochem. J.* **474**, 2235–2248 https://doi.org/10.1042/BCJ20170288

55   Pauls, E., Nanda, S.K., Smith, H., Toth, R., Arthur, J.S.C. and Cohen, P. (2013) Two phases of inflammatory mediator production defined by the study of IRAK2 and IRAK1 knock-in mice. *J. Immunol.* **191**, 2717–2730 https://doi.org/10.4049/jimmunol.1203268

56   Emmerich, C.H. and Cohen, P. (2015) Optimising methods for the preservation, capture and identification of ubiquitin chains and ubiquitylated proteins by immunoblotting. *Biochem. Biophys. Res. Commun.* **466**, 1–14 https://doi.org/10.1016/j.bbrc.2015.08.109

57   Zamyatina, A., Gronow, S., Puchberger, M., Graziani, A., Hofinger, A. and Kosma, P. (2003) Efficient chemical synthesis of both anomers of ADP l-glycero- and d-glycero-d-manno-heptopyranose. *Carbohydr. Res.* **338**, 2571–2589 https://doi.org/10.1016/S0008-6215(03)00319-7

58   Shevchenko, A., Tomas, H., Havliš, J., Olsen, J.V. and Mann, M. (2007) In-gel digestion for mass spectrometric characterization of proteins and proteomes. *Nat. Protoc.* **1**, 2856–2860 https://doi.org/10.1038/nprot.2006.468

59   Campbell, D.G. and Morrice, N.A. (2002) Identification of protein phosphorylation sites by a combination of mass spectrometry and solid phase Edman sequencing. *J. Biomol. Tech.* **13**, 119–130

60   Perez-Riverol, Y., Bai, J., Bandla, C., García-Seisdedos, D., Hewapathirana, S., Kamatchinathan, S., et al. (2022) The PRIDE database resources in 2022: a hub for mass spectrometry-based proteomics evidences. *Nucleic Acids Res.* **50**, D543–D552 https://doi.org/10.1093/nar/gkab1038